AD-781 114

GENERATION OF ULTRA-HIGH POWER ELECTRICAL PULSES

L. Birenbaum, et al

Polytechnic Institute of New York

Prepared for:

Rome Air Development Center

May 1974

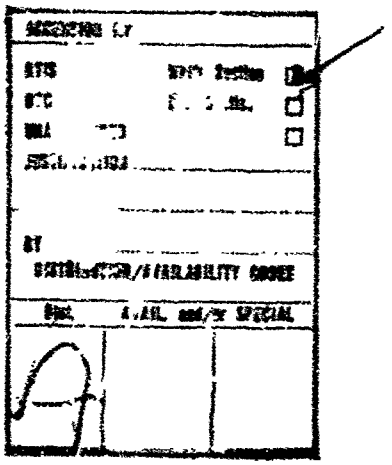

Do not return this copy. Retain or destroy.

UNCLASSIFIED

SECURITY CLASSIFICATION OF THIS PAGE (When Data Entered)

REPORT DOCUMENTATION PAGE		READ INSTRUCTIONS BEFORE COMPLETING FORM
1. REPORT NUMBER RADC-TR-74-119	2. GOVT ACCESSION NO.	3. RECIPIENT'S CATALOG NUMBER AD-781114
4. TITLE (and Subtitle) GENERATION OF ULTRA-HIGH POWER ELECTRICAL PULSES		5. TYPE OF REPORT & PERIOD COVERED Final - 1 Dec 72 - 30 Nov 73 6. PERFORMING ORG. REPORT NUMBER N/A
7. AUTHOR(s) L. Birenbaum E. Levi		8. CONTRACT OR GRANT NUMBER(s) F30602-73-C-0053
9. PERFORMING ORGANIZATION NAME AND ADDRESS Polytechnic Institute of New York 333 Jay Street Brooklyn, New York 11201		10. PROGRAM ELEMENT, PROJECT, TASK AREA & WORK UNIT NUMBERS 45060351
11. CONTROLLING OFFICE NAME AND ADDRESS Rome Air Development Center (OCTP) Griffiss AFB, NY 13441		12. REPORT DATE May 1974 13. NUMBER OF PAGES 82
14. MONITORING AGENCY NAME & ADDRESS(if different from Controlling Office) Same		15. SECURITY CLASS. (of this report) UNCLASSIFIED 15a. DECLASSIFICATION/DOWNGRADING SCHEDULE N/A

16. DISTRIBUTION STATEMENT (of this Report)

Approved for Public Release. Distribution Unlimited.

17. DISTRIBUTION STATEMENT (of the abstract entered in Block 20, if different from Report)

Same

18. SUPPLEMENTARY NOTES

RADC Project Engineer: Mr. William C. Quinn (OCTP)

19. KEY WORDS (Continue on reverse side if necessary and identify by block number)

Superconducting Compounds
Microwave
Electronics and Electrical Engineering
Electromagnetic Radiation
Electrical Machinery
RF Transmitters
Electrical Power Conversion Devices
Pulse Power
Nuclear Power Sources
Energy Storage
Conversion Techniques

20. ABSTRACT (Continue on reverse side if necessary and identify by block number)

This report is a comprehensive assessment of the state-of-the-art of various energy conversion techniques involving high power electrical pulse generation. The subjects treated include rotating machines, explosive devices, superconductivity, switching, and plasma techniques, including the supercritical temperature and pressure regions.

DD FORM 1 JAN 73 1473 EDITION OF 1 NOV 65 IS OBSOLETE

UNCLASSIFIED

SECURITY CLASSIFICATION OF THIS PAGE (When Data Entered)

FOREWORD

This report has been reviewed by the Office of Information, RADC, and approved for release to the National Technical Information Service.

This report has been reviewed and is approved.

APPROVED: William C. Quinn

WILLIAM C. QUINN
RADC Project Engineer

APPROVED: William T. Pope

WILLIAM T. POPE
Assistant Chief
Surveillance and Control Division

FOR THE COMMANDER: Carlo P. Crocetti

CARLO P. CROCETTI
Chief, Plans Office

EVALUATION

Project:	4506
Contract No:	F30602-73-C-0053
Effort Title:	High Energy Density Pulses
Contractor:	Polytechnic Institute of Brooklyn 333 Jay St Brooklyn, NY 11201

The past few years have seen considerable progress on a number of new techniques involving or related to energy storage and conversion eg explosive flux compression, cryogenics, radiating plasmas, etc. Furthermore, new approaches to older techniques have brought forth new designs aimed at new applications and higher power levels eg rotating machines, line type modulators, etc.

This effort was aimed specifically at accomplishing a comprehensive technology assessment of high power pulse generation. Various techniques are discussed in such terms as state-of-the-art, inherent limitations, future prospects, etc. It is hoped that the information provided will be of use both to the engineer involved in a single particular application and to the managing scientist concerned with long range planning in the pulsed energy field.

This effort is part of RADC Technology Plan TP05.

William C. Quinn

WILLIAM C. QUINN
Proj Engr/OCTP

Generation of Ultra-High Power Electrical Pulses

		Page
I.	Introduction	2
II.	Overview: An Assessment of Ways of Generating High-Power and High-Energy Electric Pulses	3
III.	Video Pulse Generation Methods	
	A. Rotating machinery	10
	B. Magnetic flux compression (explosive techniques)	17
	C. Electronic modulators	25
	D. Relativistic beams	27
IV.	RF Pulse Generation: high-power bursts of microwave radiation	
	A. Microwave pulse generation using relativistic electron beams	33
	B. Radiating plasmas	36
	C. Rapid release of stored microwave energy	43
V.	Parametric Studies of Pulse Generation	48
VI.	Related Topics	
	A. Switching: metallization and non-ideal plasmas	62
	B. Comments on superconductivity	69
VII.	An Acknowledgment	82

Supplementary Report:

"Plasma Instabilities as a Source of RF Power" - C. F. Carnivale — Separately bound

I. Introduction

At present, there is a great need for generators of huge electric pulses to implement current and proposed fusion experiments; to power increasingly energetic laser devices; for stationary as well as airborne radar systems; for military applications.

Recent advances have occurred in the laser and plasma fields. Breakthroughs have been achieved in the science of materials. Extensive studies are being carried out in the U. S. S. R. of non-ideal plasma states and of the metallization phenomenon. These developments make it advantageous to stop and consider the present technical status of pulse generation, and to inquire: Which would be the most profitable directions to pursue to advance the art?

This report assesses the state of the art of generating high-power, high-energy electric pulses. To accomplish this goal, it was necessary to give thought to many basic questions, such as:

(a) rotating machines: What are the present upper limits for pulse amplitude and the corresponding pulse durations?

(b) magnetic flux compression: What techniques have been used; how large are the generated pulses; what are their durations?

(c) electronic modulator technology: What is the limit of the capability for pulse generation in this area?

(d) relativistic electron beams: What techniques exist for controlling the high-voltage discharges creating these beams? What power levels have so far been attained? How have they been used for generating microwave pulses?

(e) plasma instabilities: Which plasma processes have prospects of utilization for RF pulse generation? What has been achieved so far?

These questions are addressed in the Overview (Sec. II) and in the technical sections following it (III-VI).

Pulse generation involves a number of closely related areas to which considerable attention is paid in the report. Some are:

(a) utilization of non-ideal plasmas: metallization

(b) whether and how advances in superconductor technology can be applied to pulse production.

Date for the assessment were obtained in several ways:

(a) By selected reading of current technical literature. Particular fields were chosen to be surveyed: those that we judged to be most relevant to large pulse generation. The information so obtained was condensed into a series of 10 self-contained papers (Sec. III-VII, each of which presents conceptual background in its field, together with a description of state-of-the-art developments.

(b) By visits to many important sites, as opportunity allowed, both

immediately prior to and during the contract period (examples: Los Alamos; Livermore; Princeton; Max-Planck Institute; Kurtachov Institute; Nagoya Plasma Physics Institute.) By attendance at technical conferences (examples: electronic modulators, NYC 9/73; fusion, Philadelphia APS 11/73). By conversations in depth with people expert in various fields.(See Sec. VII.) The perspectives and insights gained in this way served as background for the technical papers, and were incorporated into the Overview.

II. Overview: An Assessment of Ways of Generating High-Power and High-Energy Electric Pulses

Electric pulses with energies approaching the gigajoule range and powers on the order of tens of terawatts are increasingly finding use in weapons systems, research, and industry. Among the various important applications are plasma and laser technologies, oil prospecting, geological and oceanographic surveying, and metal cutting and welding.

A. Recent Advances in Materials

The development of new devices usually involves two major aspects: (1) materials, and (2) design. Since technical and economic considerations impose limits on the dimensions of the pulse generator, high energy and power outputs imply high energy and power densities, and hence, high mechanical, electromagnetic, and thermal stresses in the materials employed. Fortunately, recent advances in the science of materials, at extremes of both low temperature and high pressure, hold promise for attaining the required performance parameters.

In our earlier studies of electromechanical pulsers [1-4], it was suggested to "freeze" the impressed magnetic field in a superconducting shield, in order to reduce the rise time of the pulse and enhance the overall efficiency. This, however, could only be done if superconductors were produced in twisted multistrand filament form, so as to reduce the ac losses associated with the current pulse. Such an ideal shield can now be realized, since niobium carbonitride has successfully been converted into intrinsically stable superconducting flexible fibers with a critical temperature in excess of 18°K [5].

Moreover, the new fibers will allow practical realization of a novel type of pulse generator. According to Thomassen [6], a system of three nested spherical coils, made of superconducting material, can be used to transfer 150 MJ of energy to an inductive load in a time of about 10 msec.

Great progress has also been made in understanding the behavior of materials near critical temperatures and pressures, conditions which are likely to prevail in electromechanical pulsers. Under the concommitant action of strong electric fields and shock compression, insulating materials, such as the inert gases filling the generators, may acquire metallic conductivities [7]. This metallization phenomenon poses a double challenge to the designer of electromechanical pulsers:

(1) How to avoid the creation of short-circuited paths, which may shunt the load or change the impedance matching characteristics of the connecting transmission lines.

(2) How to utilize these metallization effects in a constructive way.

The combination of metallic-state conductivities with the low viscosity and consequently, the high-operating velocities afforded by the gaseous state is ideally suited for impulsive, magnetofluid dynamic generation schemes [8,9]. The high conductivity and high flow-velocity can also be utilized for the realization of high-power, fast-acting switching elements.

B. Video Pulse Generator Classes

Pulse generators fall into four major classes, which are distinguished by their pulse duration, energy storage form, and design.

1. Electromechanical Pulsers with Kinetic Energy Storage

These pulsers cover the longest pulse range (down to tens of milliseconds), with efficiencies of better than 50 percent. Levi and Pande [1-4] have studied both the homopolar and the heteropolar types. A recent realization of the former type by Rioux [10] yields a 100 MJ output in several tenths of a second. Pulses one order of magnitude shorter, with an output energy of 15 MJ, are obtained from the Rebut-Torossian generator [11]. This design makes use of a structure similar in function and concept to the shield of Levi and Pande [12].

2. Explosive-Driven Pulse Generators

These cover the pulse range between a fraction of a millisecond and a few microseconds. The energy stored in chemical form is used directly to propel the conductor against the self-excited magnetic field [13-14]. The overall efficiency is on the order of a few percent, and the generator is destroyed after a single shot. These generators, however, are relatively cheap (less than $500 per MJ output), and very compact (up to 100 MJ within the dimensions of one cubic meter). They have performed reliably in outer space [15] and can penetrate the highest magnetic fields [16-17]. In 1966 Sakharov [18] disclosed the attainment of 25 MG fields. Much higher fields have been attained more recently [19]. It is interesting to note that the corresponding magnetic pressures exceed 10^6 atm. A possible application of such generators, as suggested by Sakharov [18], is a betatron accelerator capable of delivering bursts of 10^{18} protons at 1000 GeV energy. He calculates that the experiment could be repeated 50 to 100 times for the cost required to build a permanent accelerator.

3. Pulse Generators with Intermediate Inductive Energy Storage

Inductive energy storage has already been mentioned in connection with Thomassen's design [6]. It is also used in cascaded explosive-driven generators [20] in order to shorten the rise time of the pulse to the order of 1 μsec. A major drawback of interstage inductive storage is the necessity of using an opening switch in order to transfer the energy to the load. The transfer efficiency is often much less than 50%. Presently used as switching elements are explosive wires and foils. Faster rise times, but not higher efficiencies, could be obtained as mentioned before, by utilizing the rapid changes in conductivity which accompany the transition from metallization to the gaseous state.

4. Pulse Modulators with Capacitive Energy Storage

Capacitor banks are the only energy source capable of delivering sub-microsecond pulses with efficiencies better than 80%. However, since the density of stored energy is three orders of magnitude less than in rotating machines, and five orders of magnitude less than in chemical explosives, the energy output is limited to tens of MJ's. A promising development in this area is the use of water as a dielectric. Taking advantage of the high dielectric constant ($\epsilon \approx 80$) and high dielectric strength ($E_{max} \approx 500$ kv/cm), energy densities approaching 1 MJ/m^3 could be attained. For pulsed output applications, the high conductivity of water and consequent losses would not be objectionable.

C. RF Pulse Generation

The number of ways of generating high-power RF or microwave pulses is far more limited than for video pulses.

1. Conventional means Conventional means of generating high-power microwave pulses utilize interaction of an electron beam (confined within a vacuum envelope) with slow-wave or resonant structures. In this class may be placed the magnetron; amplitron; klystron; backward wave oscillator; travelling wave tube. Some general limitations on the powers available from these conventional sources are [21, 22]:

(a) Electrical breakdown at the window connecting the source to the antenna system.

(b) Heat dissipation in the associated slow wave or resonant structures.

(c) Admissible current density of the cathode. One technique that sometimes serves to by-pass this limitation, especially at millimeter wavelengths, is the use of an electron focussing gun which multiplies the cathode current density by a factor of about 50.

(d) Admissible voltage. This limitation is particularly important under the pulsed conditions of interest in this context. For voltages in excess of 40 kV the electron velocity approaches the speed of light and RF voltages produce variation in mass, rather than the necessary velocity modulation. However, the limiting voltage may well be on the order of 150 kV if it is desired to obtain bandwidth in excess of 30%. Bandwidth appears to be limited by dispersion of the slow wave structures. When the phase velocity approaches the speed of light, low dispersion and high coupling impedance seem to be incompatible.

(e) Coherence of oscillations. For a given beam current density, the number of electrons decreases as the cube of the wavelength. As the wavelength decreases toward 1 mm, coherent oscillations become increasingly difficult to achieve.

2. Non-conventional Means Recent investigations using relativistic pulsed beams of electrons have opened a new avenue to the generation of high-power RF pulses. High voltage - high current - 100 n sec discharges at the terawatt level can now be generated and controlled [23]. By placing suitable rigid periodic structures [24] in a position to couple to the beam, or by

allowing the beam to interact with magnetic fields with fixed spatial periodicity [25], pulses of narrow-band energy have been generated. The dominant frequency is controlled by the spatial period. Power levels of 1 GW [26] have been attained in the X-band microwave range for pulse durations somewhat shorter than that of the video pulse discharge.

Bursts of RF radiation with black-body spectral distribution were generated by Cowan and Freeman [27] using an arc discharge in a deuterum plasma. Peak powers in the order of terawatts with energies in the order of megajoules were obtained. Here, the energy conversion process from chemical to electromagnetic form was a direct one.

Each of these methods of RF pulse generation has a different virtue: one has a narrow spectral range but low power, where as the other has a broad spectrum but enormous power. This comparison suggests that attempts should be made to channel the high powers inherent in plasmas into narrow spectral ranges by properly utilizing the plasma processes naturally giving rise to monochromatic radiation.

To summarize technical developments in the area of pulse generation, we offer Table I, optimistically titled, "The State of the Art at a Glance."

In conclusion, high-energy, high-power pulse generation is an active field of endeavor in which development of both materials and design is keeping pace with increasingly demanding requirements.

Pulse Generation

The State of the Art at a Glance

Mode	Pulse Duration	Energy/ Pulse	Power Level	Appli-cation	Comments	See Report Section
Single Rotating Machine	.01 sec	15 MJ	1.5 GW	CTR	Under construction. Designed by Rebut-Torossian	III A
	~.2 sec	100 MJ	0.5 GW	CTR	Under construction. Designed by Rioux. Homopolar machine	
	~.01 sec	150 MJ	15 GW	CTR	Proposed scheme by Thomassen Nested spherical superconducting coils.	
Many synchronized machines	5 sec	960 MJ	192 MW	CTR	Princeton plasma physics labs. Used as supply for Tokomak 12 generators	III A
Explosive Flux Compression	100 μsec rise time	5 MJ		Plasma studies	"Off-the-shelf" item at Los Alamos	III B
	3 μsec rise time	~1 MJ			Uses exploding wire + dielectric breakdown switch to achieve 3 μsec	
Electronic Modulator	20 μsec (200 pps)	40 kJ	2GW	CO_2 Laser pulsing	A proposed design by Pruitt, RCA.	III C
High voltage Discharge	~100 n sec	2 MJ	20 TW	EMP studies? CTR?	Uses "Aurora" device at Diamond Labs, MD	III D
Relativistic beam + periodic B field + waveguide	70 n sec	70 J	1GW		X band - Granatstein et al. Based on experiments by Friedman and Herndon at NRL.	IV A

(CTR = Controlled Thermonuclear Research)

REFERENCES

1. E. Levi, "Electromechanical Pulse Generators," Proc. 6th Symp. on Hydrogen Thyratrons and Modulators, Ft. Monmouth, N.J., 250-277 (1960).

2. H. Pande, "Linear Analysis of the Electromechanical Pulser," Trans. AIEE, Part I, 309-315 (July, 1961).

3. E. Levi, "Electromechanical Pulsers with Solid Conductors," Paper No. CP64-108, presented at the IEEE Winter Power Meeting, New York, N.Y. (February 2-7, 1964).

4. H. Pande, "Current Source Excitation Type Electromechanical Pulser," IEEE Trans. on Communications Electronics, No. 74, 528-535 (September, 1964).

5. Research and Development Management Report, TA-AFML-1107-73-02 (August, 1972).

6. K. I. Thomassen, "Reversible Magnetic Energy Transfer and Storage Systems," Los Alamos Scientific Lab., U. of California, Informal Report LA-5087-MS VC-20 (November, 1972).

7. F. V. Grigorév, S. B. Kormer, O. L. Mikhailova, A. P. Tolokho and V. D. Urlin, Zh. E. T. F. Pis. Red. 16, 286-290 (1972). (English Translation in Sov. Phys. JETP Letters, 16, 201-204 (1972).

8. E. Levi and M. Sandler, "An Approach to Unsteady One-Dimensional Magneto-Gas Dynamic Problems," Teplofizika Visokikh Temperature, 2, No. 3, 351-358 (May-June, 1964). (English Translation in High Temperature, 2, 318-327 [1964]).

9. E. Levi and M. Panzer, "Electromechanical Power Conversion," (New York: McGraw-Hill, 1966). [Russian Translation "Mir" (Moscow, 1969).]

10. J. Chaboseau, "La Generatrice Impulsionelle Rioux de 100 Megajoules," in an undated issue of Techniques Cie Electro-Mechanique (pages 17-21).

11. J. Delassus, "Une Nouvelle Solution aux Problemes Impulsionelles; La Pulsatrice Rebut-Torossian," in an undated issue of Techniques Cie Electro-Mechanique (pages 12-17).

12. E. Levi and H. Pande, "Electromechanical Pulsers," Tech. Documentary Report No. RADC-TDR-63-436 (April 1964). AD# 601 714

13. J. W. Shearer, et al. "Explosive-Driven Magnetic Field Compression Generators," J. Appl. Phys., 39, No. 4, 2102-2116 (March, 1968).

14. J. C. Crawford and P. A. Damerow, "Explosively Driven High Energy Generators," J. Appl. Phys., 39, No. 11, 5224-5231 (October, 1968).

15. C. M. Fowler, D. B. Thomson, W. B. Garn and R. S. Caird, "M.-16 Summary Report. The Birdseed Program" Los Alamos Scientific Lab, U. of California, Informal Report LA-5141-MS (July 1970).

16. H. Knoepfel, "Pulsed High Magnetic Fields" (Amsterdam: North Holland-American Elsevier, 1970).

17. C. M. Fowler, "Megagauss Physics," Science, 180, No. 4083, 261-267 (1973).

18. A. D. Sakharov, Usp. Fiz. Nauk, 88, 725-734 (1966). [English Translation in Sov. Phys. Usp. 9, No. 2, 294-299 (1966).]

19. Private communication.

20. D. B. Cummings, "Cascading Explosive Generators with Autotransformer Coupling," J. Appl. Phys., 40 No. 10 (September, 1969).

21. O. Doehler, "Traveling Wave Tubes," Proc. of the Symposium on Electronic Waveguides. Microwave Research Institute Symposium Series, Vol. VIII, Polytechnic Press, Brooklyn, N.Y. pages 1-19, (1958).

22. A. F. Harvey, "Microwave Engineering," Academic Press, (1963).

23. D. L. Morrow, et al, "Concentration and Guidance of Intense Relativistic Electron Beams," Appl. Phys. Lett. 19, No. 10, 441-443, (15 Nov. 1971).

24. J. A. Nation, "On the Coupling of an High-Current Relativistic Electron Beam to a Slow Wave Structure," Appl. Phys. Lett. 17, No. 11, 491-494, (1 Dec. 1970).

25. M. Friedman and M. Herndon, "Emission of Coherent Microwave Radiation from a Relativistic Electron Beam Propagating in a Spatially Modulated Field," Phys. Rev. Lett., 29, No. 1, 55-58, (3 July 1972).

26. V. L. Granatstein, et al, "Gigawatt Microwave Emission from a Highly Relativistic Intense Electron Beam," Bull. Amer. Phys. Soc., 18, No. 10, 1354-1355, (Oct. 1973).

27. M. Cowan and J. R. Freeman, " Explosively Driven Deuterium Arcs as an Energy Source," J. Appl. Phys., 44, No. 4, 1595-1603, (April 1973).

III. Video Pulse Generation Methods

A. Video Pulse Generation using Rotating Machinery

Some recent papers concerned with generation of pulses by rotating machinery are reviewed. The goal is to present state-of-the-art achievements in high-energy pulse generation as viewed against a background of what may reasonably be expected in this area.

1. In order to analyze electromechanical pulsers from a general point of view, Pande and Levi chose as a model the following: a moving short-circuited coil magnetically coupled to a stationary excited coil, with a coupling coefficient that varied with the motion [1, 2, 3]. They found that the rise time of the pulse, as determined by the leakage inductances, could be reduced by orders of magnitude if appropriate shielding was employed.

Fig. 1 is intended to illustrate the shielding mechanism. A short-circuited coil (armature) is shown moving through a magnetic field created by a stationary field structure. (In an ordinary machine, one might expect to find the field structure on the rotor.) The shield is shown as a thin cylinder between the two.

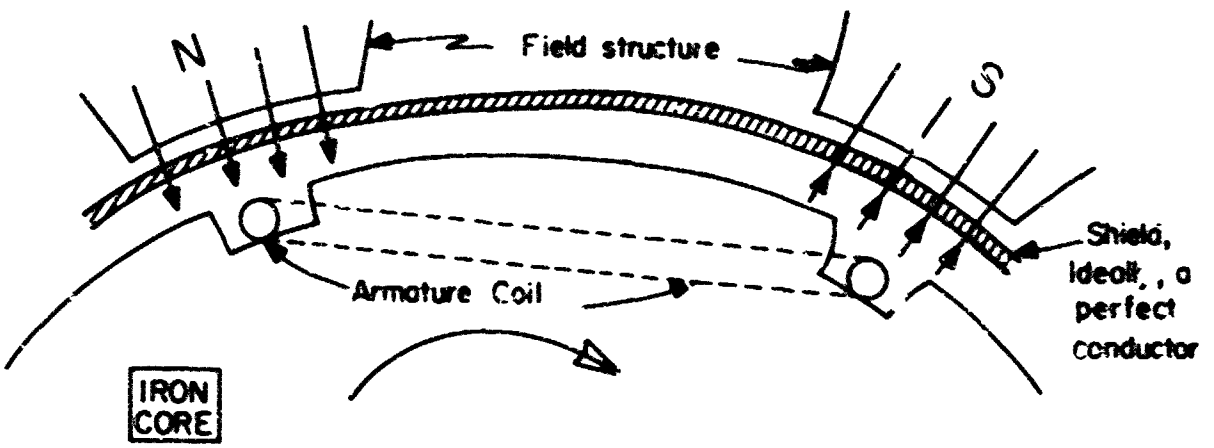

Fig. 1 Illustrating the mechanism of a shield that reduces pulse rise time

Within the material of the shield, ideally a perfect inductor, the electric field E has to be zero. This implies that $\partial\phi/\partial t$ also has to be zero within any closed loop inside the shield. Hence, the flux lines produced by the field structure are "frozen" with the shield. In addition if the rotating coil is taken to be an ideal conductor, then E is zero within the coil material. As a consequence, over the surface spanned by the rotating coil, $\partial\phi/\partial t = 0$.

If the flux initially interlinked with the coil is zero, it must remain so. Hence the currents induced in this rotating winding are a forced response to the magnetic fields created by the stationary structure, as seen by the rotating coil. The induced currents have to be large enough to create a flux which will cancel that of the stationary field structure. The rise time of these current pulses is limited by a) the degree to which the magnetic lines can be spatially arranged to simulate a step function, b) the rotational velocity of the coil (about 200m/s) and c) departures from the idealized model arising from less than perfect coupling of the coils (leakage inductance). An analysis of typical situations suggests that pulses of one millisecond duration, of power level 100MW/(meter^3 of armature coil material) is a good feasibility estimate for this method of pulse generation [3].

2. J. Delassus [4] has described in detail a pulse generator designed by Rebut and Torossian for application to controlled nuclear fusion plasma studies. The field structure is mounted on the rotor. Also fixed to the rotor, and shielding it from the stationary armature surrounding it, is a structure similar in function and concept to the shield of Pande and Levi; in appearance, it resembles a squirrel-cage rotor of an ordinary induction motor. The field excitation is provided initially by a battery through slip rings (refer to Fig. 2 from Delassus) and then by self-excitation (K_2 closes) through an auxiliary stator winding and rectifier back to the rotor. The principal winding on the stator is connected to the load circuit (K_3 closes) when the flux threading through the winding reaches a maximum (as does also the associated energy storage). Finally, the load circuit is isolated from the machine (K_4 closes) when the current pulse reaches its maximum. For this cleverly-designed, pulsed-mode model, test results were deemed excellent:

pulse energy - 500kJ

(peak) excitation curren
5400A

(peak) magnetic field -
24kG

field buildup time -
0.2 sec

(specs for) drive motor -
45kW, 1500RPM

ruggedness - excellent

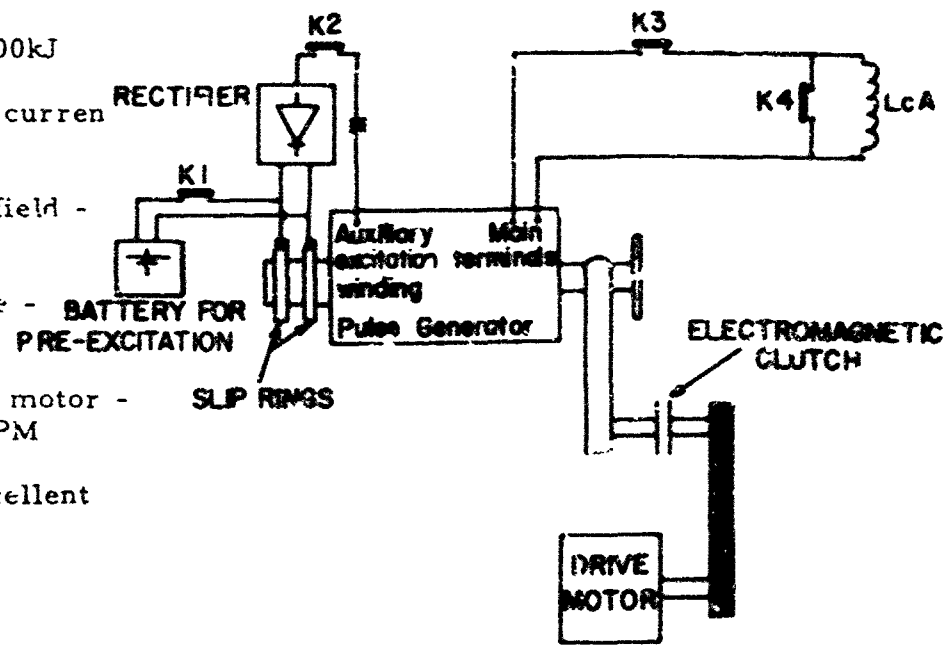

Fig. 2 Diagram showing some aspects of the 500kJ prototype of the Rebut-Torossian Pulse Generator

Extrapolation of this model to one 30 times more powerful leads to a pulse power of 15MJ with a 0.01 sec rise time. Four of these machines would more than suffice, when operated in parallel, to supply all planned fusion plasma experiments. One of these machines is being built in Milano by Brown-Boveri for use in the EURATOM-CNEN Laboratory of Frascati for energizing their Tokomak machine.

3. J. Chaboseau [5] describes the construction details of a 100MJ pulse generator of the homopolar type, designed by Rioux, and also intended for controlled nuclear fusion studies. It is now being built at the CEM Bourget plant. A 5MJ prototype has already been tested. The essential features of the 100MJ machine are shown in the figures below, taken from Chaboseau's paper:

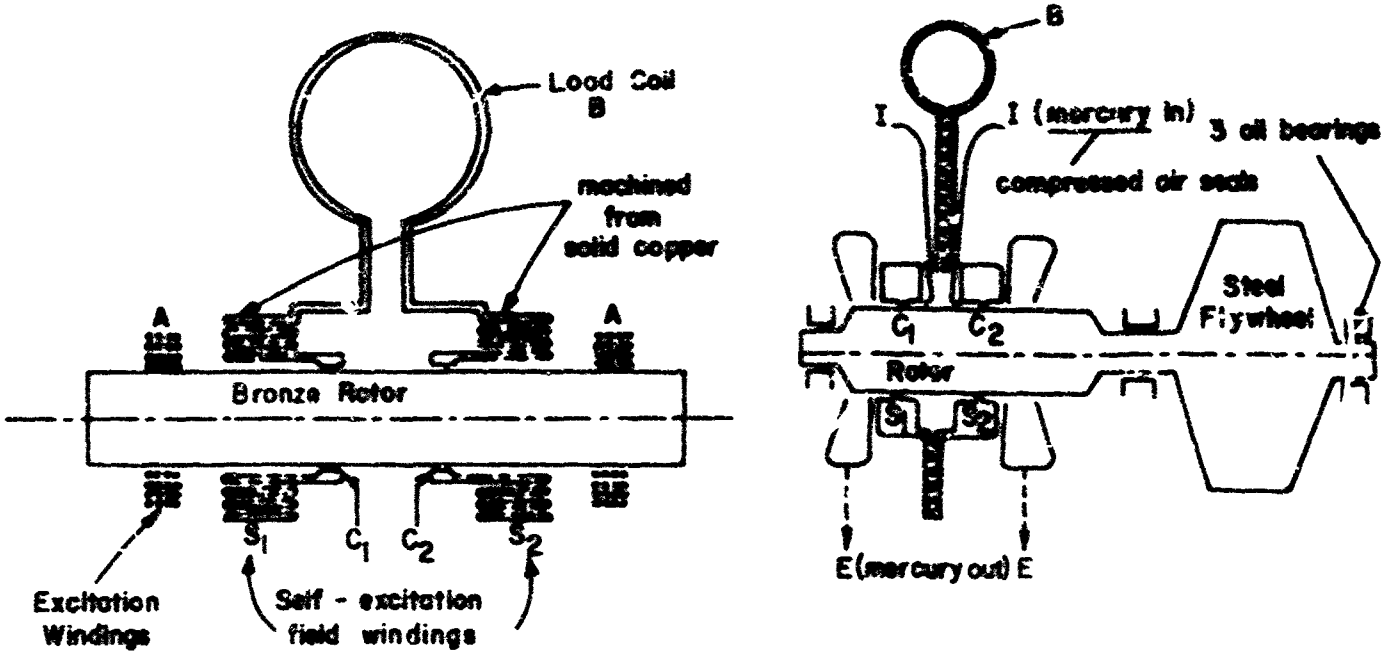

Fig. 3 Some Features of the Rioux Homopolar Pulse Generator (100MJ)

An auxiliary drive motor brings the rotor and flywheel up to speed, and the clutch is disengaged. The excitation windings A are energized. Then, the mercury contacts C_1, C_2 are closed. This initiates a buildup of current in the load coil B, as a result of auto-excitation of the field windings S_1, S_2 in series with B. Pulse decay occurs as the machine is slowed by very strong electro-magnetic braking forces. As in the Rebut-Torossian machine, all the energy is initially in kinetic form, here stored in the flywheel. Technical problems associated with its realization are indeed formidable and are described in the paper. Pulse duration is several tenths of a second.

4. Thomassen [6] proposes an extremely interesting design, also for CTR plasma studies, intended to transfer energies of 150 MJ to an inductive

load in a time of about .01 second. The basic idea is now described, and typical design figures are given: Three nested spherical coils made of superconducting material are used, (see Fig. 4) with coil 1 stationary, permitting the creation of a 60kG field. Coils 2 and 3 rotate, but are fixed with respect to each other with their magnetic axes 90° apart. Hence, no mutual coupling between 2 and 3 exists. If the system is excited initially with coil 3 axis aligned with that of 1, currents flow in coil 3 but not in coil 2. If the inner coils (2, 3) are now rotated, energy is transferred from 3 → 2 and 2 → 3 cyclically. Proper choice of parameters permits rotation without application of torque. So far, the arrangement is interesting but not useful for energy transfer.

If coil 3 is not short-circuited, but instead is closed through an intermediate transformer for coupling to the load L_4 (see Fig. 4), a means is available for energy transfer. Thomassen choses parameters for a 140MJ transfer to L_4 based on the criteria: no rotational torque under steady rotation; coil and transformer coupling coefficients as large as possible; maximum energy transfer (62%) to L_4; B_{max} = 60kG. He finds R_1 = 1.47m, R_2 = 1.17m, R_3 = 1.42m and specifies inductances and other parameters.

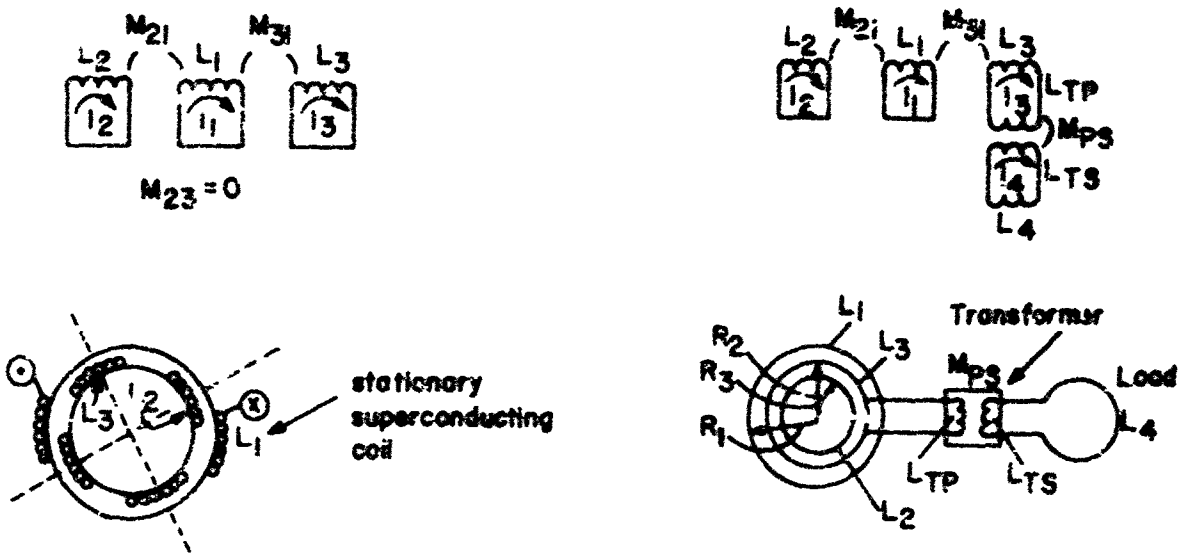

Basic Idea

How to transfer energy to load L_4

Fig. 4 Thomassen Pulse Generator

The problem with this system is the large energy requirement in accelerating the system from rest, and then stopping it. The narrower the pulse desired, the higher is this energy requirement, of the order 55MJ for a .01 second pulse.

5. At the present time, the largest rotating machine pulse generator in the U.S. is located at the Princeton Plasma Physics Laboratory. It served as the power supply for the stellarator machine, and now pulses the Tokomak machine to which the stellarator was converted. It consists of 12 generators, each of which (coupled to its motor and flywheel) supplies 16 MW for 5 seconds at 800 V. The total pulse power is 192 MW for 5 seconds, with a corresponding energy of 960 MJ.

REFERENCES

1. H. C. Pande, "Linear Analysis of the Electromechanical Pulser," Nov. 1960, RADC-TN-61-55. *AD# 254 363*

2. E. Levi, "Electromechanical Pulsers," Tech. Documentary Report No. RADC-TDR-64-109, May 1964 *AD# 601 569*

3. H. C. Pande, "Electromechanical Pulsers," Tech. Documentary Report No. RADC-TDR-63-436, April 1964. *AD# 601 714*

4. J. Delassus, "Une nouvelle solution aux problemes impulsionnels: La pulsatrice Rebut-Torossian," in a recent issue of Techniques Cie Electro-Mecanique (pages 12-17).

5. J. Chaboseau, "La generatrice impulsionelle Rioux de 100 megajoules," in a recent issue of Techniques Cie Electro-Mecanique (pages 17-21).

6. K. L. Thomassen, "Reversible Magnetic Energy Transfer and Storage Systems," Los Alamos Scientific Lab, Univ. of California, Informal Report LA-5087-MS, UC-20, Nov. 1972.

Symbols Used

$i_{1,2,3}$	current in coils 1, 2, 3 (A)
t	time (s)
B	flux density
$L_{1,2,3}$	inductance of coils 1, 2, 3 (H)
L_4	load inductance (H)
L_{TP}, L_{TS}	inductance of transformer primary, secondary (H)
$M_{12,13,23}$	mutual inductance (H)
M_{PS}	mutual inductance, primary, secondary (H)
$R_{1,2,3}$	resistance of coils 1, 2, 3 (Ω)
ϕ	flux (Wb)

III. B. Video Pulse Generation by Magnetic Flux Compression

1. Basic Idea

A simple model for an implosive pulse-generating device, helpful in later discussion, is the following. A perfectly-conducting, hollow cylinder of length ℓ and inner diameter D, has within it a longitudinal uniform magnetic field B_o.

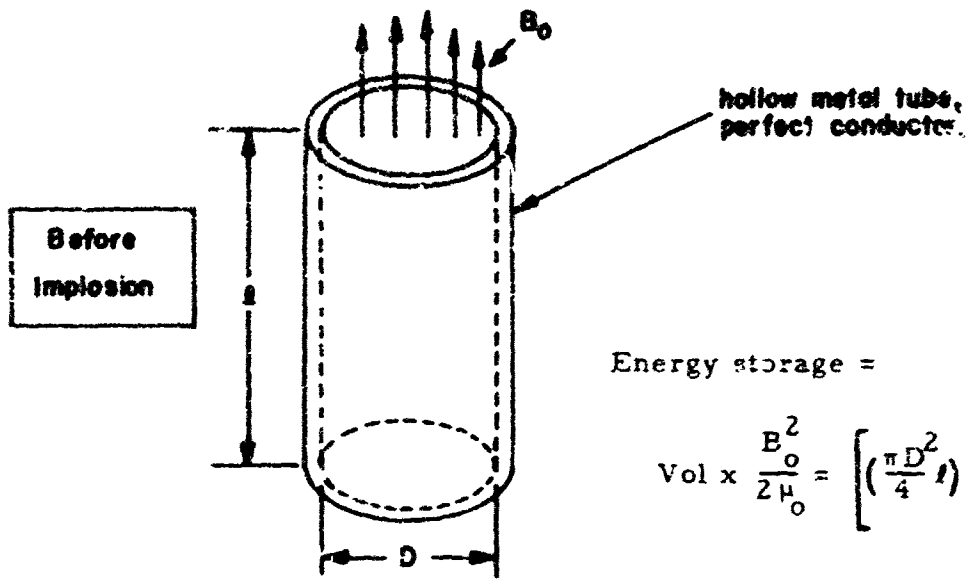

Energy storage =

$$\text{Vol} \times \frac{B_o^2}{2\mu_o} = \left[\left(\frac{\pi D^2}{4}\ell\right)\frac{B_o^2}{2\mu_o}\right]$$

Implosion occurs. The flux $\iint \underline{B}\cdot \underline{n}\, dA = \phi$ within the cylinder is constrained to remain constant because electric field $\underline{E}$ within the conductor is zero: $\oint \underline{E}\cdot \underline{d\ell} = -\frac{\partial \phi}{\partial t} = 0$ implies ϕ = constant. Energy multiplication in this ideal case is then $\left(\frac{D}{d}\right)^2$. The energy in excess of the original comes from compression of the tube against the outward radial magnetic pressure $\frac{B^2}{2\mu_o}$.

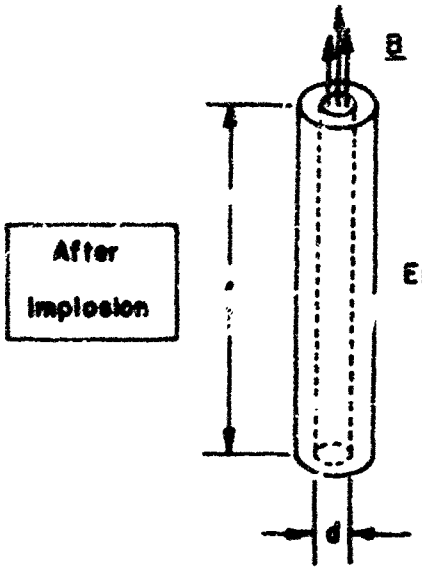

$$B_0\left(\frac{\pi D^2}{4}\right) = B\left(\frac{\pi d^2}{4}\right)$$

$$B = B_0\left(\frac{D}{d}\right)^2$$

$$\text{Energy storage} = \text{Vol} \times \frac{B^2}{2\mu_0} = \left(\frac{\pi d^2}{4}\,\ell\right) \times \left(\frac{B_0^2 \left(\frac{D}{d}\right)^4}{2\mu_0}\right)$$

$$= \left[\left(\frac{\pi D^2}{4}\,\ell\right)\frac{B_0^2}{2\mu_0}\right] \times \left(\frac{D}{d}\right)^2$$

With an ideal model in mind (infinite conductivity), in circuit terms, the initial (o) and final (f) states of the system are related thus:

$$\Phi_o = \Phi_f = L_o I_o = L_f I_f$$

$$W_f = \frac{1}{2} L_f I_f^2 = W_o \frac{I_f}{I_o} = W_o \frac{L_o}{L_f}$$

This model does not include the manner in which energy is transferred from the generator to a load. However, this does emerge from the following brief discussion of the structural features and performance of practical devices.

2. Practical Devices

a) The "bellows generator" of Knoepfel et al [1] is shown in the two figures reproduced from their paper. In Fig. 1, an initial magnetic field B_o (into the paper) is established by discharging a capacitor bank into the generator through coaxial cables. Detonation, initiated at the left, forces the two conducting central plates (liners) to close the loop (i.e., into the positions shown by the dotted lines), trapping B_o, and then compressing it into the load solenoid at the right. Fig. 2 shows a specific generator, device 121, which uses 13 pounds of explosive to deliver 0.9 MJ into the single turn 12 nH load coil. After flux compression starts, it takes about 100 μ seconds to establish a maximum B of 0.7 MG and a maximum I of 12.5 MA. The initial current I

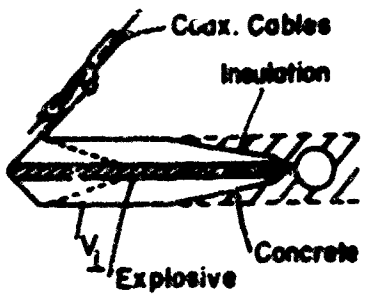

Fig. 1. Typical bellows generator

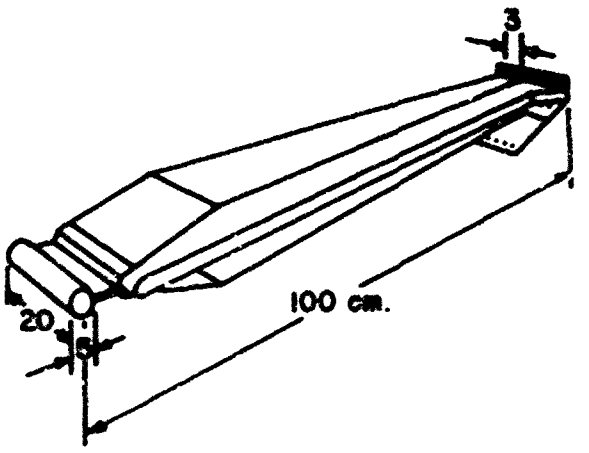

Fig. 2. Device type 121

is about .55 MA. The conversion efficiency from chemical to magnetic energy is equal to 3%.

b) Crawford and Demerow [2] describe a highly-developed realization of a helical-coil flux compression generator (model 129). The two figures taken from their paper show the coaxial construction and suggest the physical changes during the explosion. A longitudinal magnetic field B_o is established

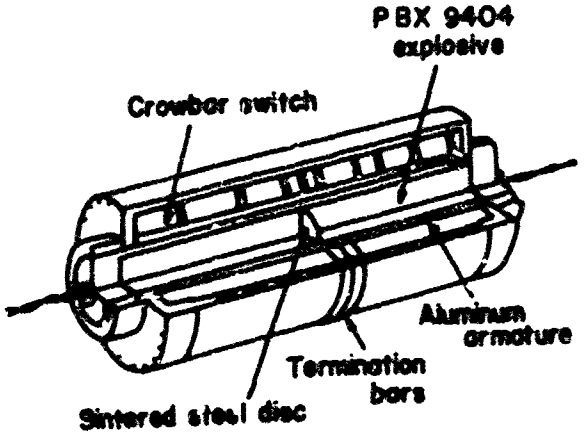

Fig. 3. Cutaway view of the 129 explosive generator.

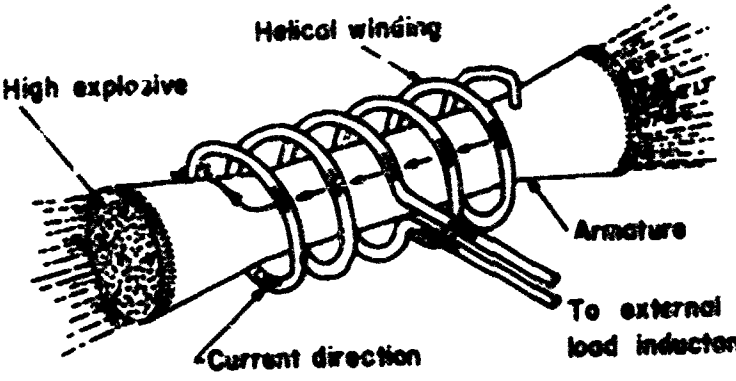

Fig. 4. Schematic drawing of the basic design used in double-ended helical generators. The armature is shown as it initially strikes the crowbar switches at each end of the generator.

inside the hollow cylindrical space between the aluminum center conductor and the helical copper outer conductor. This is done by discharging a capacitor bank through the coil, creating a current which rises to about 0.1 MA. Then, the 17 pounds of explosive within the center conductor are detonated to trap (the function of the crowbar switches) and subsequently compress the flux.

The dimensions of the device and its performance into a load inductance of 70 nH are as follows: Rise time to peak of pulse 44 μ seconds; i_f = 6.6MA; W_f = 1.5 MJ; B_f = 1 MG; conversion efficiency = 4%; outer dimensions 9" D x 18" long. The current rise is nearly exponential with a time constant of approximately 7 μ sec.

c) Shearer et al [3] describe design 10, of very similar construction, supplying 10 MA to an 80 nH load (4 MJ at pulse peak). Rise time = 130 μ seconds; initial current about .05 MA; time constant of the exponential current rise = 10 μ sec. Outer dimensions about 21" D x 30" long; same explosive; center conductor of copper; outer conductor of aluminum.

For the general class of explosive generators, Knoepfel et al [4] have made a cost estimate of $200 per MJ per shot.

With switching techniques, using exploding wires or foils and dielectric breakdown switches, it is possible to delay the delivery of energy to the load until nearly the peak of the explosion has been reached. A 3 μ second rise time [2] has been reached in this way.

Insight into the performance limitations of these flux compression devices can be obtained by introducing realistic modifications into the basic picture.

3. Effects of Finite Conductivity

The simple flux compression picture that follows from the model presented earlier is changed in very important respects by the existence of finite conductivity σ. These are now discussed qualitatively.

In the ideal case ($\sigma = \infty$) there are surface currents flowing on the inner surface of the tube of value $K = \frac{B}{\mu_o}$ amperes/meter of length. There is 0 penetration into the metal. In the practical case, these currents do penetrate the conductor with characteristic skin depth (for a planar model) of

$$\delta = \sqrt{\frac{\tau}{\mu_o \sigma}}$$

where τ is the time constant describing the exponential rise of B during the implosion. An order of magnitude for δ is

$$\tau = 10\,\mu\text{sec}$$
$$\mu_o = 4 \times 10^{-7}\ \text{H/m} \qquad \Longrightarrow \qquad \delta \approx 0.4\ \text{mm}$$
$$\sigma = 4.8 \times 10^{7}\ \text{mho/m (Cu)}$$

High values of B produce large sheet currents that flow through the surface resistive layer, producing heat dissipation. In fact, for B = 0.8 MG, the surface starts to melt, and for B = 1.5 MG, surface vaporization starts [5].

Penetration of surface currents into the metal implies that the magnetic flux also diffuses into the metal. Flux compression ratios are therefore not as high as expected. This effect is enhanced during implosion by heating of the metal, since the resulting decrease in conductivity gives a greater penetration depth δ.

These considerations raise basic questions: How does diffusion of flux into the metal affect maximum attainable B? How does melting and vaporization at the surface affect maximum attainable B? How does conductor velocity (0.1 - 1 cm/sec [5]) compare with the rate of field diffusion into the metal? At the pulse peak, the core pressures are very high ($P_{\text{kilobar}} = 39.3\ B^2_{\text{Megagauss}}$). If vaporization of the copper or aluminum conductor surface occurs, is it possible that the vapor undergoes non-metal to metal phase transitions at the core, similar to those that have been observed with mercury [6] and cesium [7] vapors? (See also Sec. VI A.) If so, this may affect energy transfer to the load. When fields are very high, do the hydro-dynamic instabilities [5] which may develop at the conductor surfaces influence the maximum attainable energy?

These factors have been separately and extensively studied. However, no definitive statement can be made about the most effective means of by-passing the limitations imposed by each.

4. Pulses Presently Attainable by Flux Compression

In conclusion, we wish to present device performance representing the present state of the art.

Helical coil devices such as those of Shearer et al [3] described earlier may be expected to deliver, reliably, pulses in the 5 MJ range to a load (~80 n H) in a single stage with a rise time exceeding 100 microseconds. In general, with such helical devices, current amplifications of 200 are easily attained with accompanying energy amplification of 70 (Shearer et al. design [10]). Inductance is relatively large, allowing one to work into a variety of loads. For comparison, bellows devices [4] have representative current amplifications of 40 with accompanying energy multiplication of 24. Inductance is relatively small, so that loads are limited to small inductances or single-turn solenoids.

With some sacrifice in energy, switching may be utilized with coaxial devices to reduce the rise time seen by the load to 3 μsec [2,4].

As an aside, the initial "seed" fields or currents can be established using energy stored in capacitor banks, with an energy transfer efficiency of the order of 70%. The subsequent transfer of chemically-stored energy into electrical form via explosive flux compression is achieved [4] with efficiency of the order of 10%.

Special coaxial configurations have been utilized at Livermore [3, 5] to create (in 2 stages) a toroidal magnetic field with 30 MJ energy and 250 MA at pulse peak (L ~ 1 nH load). Initial fields and currents were supplied by helical coil generators.

Magnetic fields of 3.3 MG have been obtained by Shearer et al [3] in their coaxial generators; 5.1 MG by Garn et al [8] using a cylindrical compression system, and measured using Zeeman splitting of the N_a 5893 Å line; 5-6 MG by the Frascati group in 1967 [5]; 14 MG, perhaps, in the Soviet hydrogen metallization experiments [9] involving pressures up to 8 megabars; 25 MG fields have been reached once or twice, it is reported by Sakharov et al [10, 11]. The overall subject of megagauss fields has been reviewed by Fowler [12]. It is probable that fields exceeding 25 MG have been achieved by this time despite the enormous pressures (~ 25 M bar) that must be overcome.

REFERENCES

1. Knoepfel, H., et al, Generation and Switching of Magnetic Energies in the Megajoule Range by Explosive Systems, Review of Scientific Instruments, Vol. 40, No. 1, pages 60-67, Jan. 1969.

2. Crawford, J.C. and Damerow, R.A., Explosively Driven High-Energy Generators, Journal of Applied Physics, Vol. 39, No. 11, pages 5224-5231, October 1968.

3. Shearer, J.W., et al, Explosive-Driven Magnetic-Field Compression Generators, Journal of Applied Physics, Vol. 39, No. 4, pages 2102-2116, March 1968.

4. Knoepfel, H., et al, Merits and Limitations of Explosively Driven Current Generators in Fusion Research, presented at 6th Symposium on Fusion Technology, Aachen, Sept. 22-25, 1970.

5. Knoepfel, H., Pulsed High Magnetic Fields, North-Holland Publishing Co., pp. 3; 184; 221-ff ; 199; 127-239. A superb source of information. 1970

6. Hensel, F. and Franck, E.V., Metal-Nonmetal Transition in Dense Mercury Vapor, Reviews of Modern Physics, Vol. 40, No. 4, pages 697-703, Oct. 1968.

7. Alekseev, V.A., et al, Soviet Physics Uspekhi, Vol. 15, pages 139-158, in English Translation, 1972.

8. Garn, W.V., et al, Technique for Measuring Megaguass Magnetic Fields Using Zeeman Effect, Review of Scientific Instruments, Vol. 37, No. 6, pages 762-767, June 1966.

9. Grigor'ev, F.V., et al, Experimental Determination of the Compressibility of Hydrogen at Densities of 0.5-2 g/cm^3. Metallization of Hydrogen. JETP Letters, Vol. 16, No. 5, pages 201-204, (in English Translation), Sept. 5, 1972.

10. Sakharov, A.D., et al, Magnetic Cumulation, Soviet Physics - Doklady, Vol. 10, No. 11, pp 1045-1047, (in English translation), May, 1966.

11. Sakharov, A.D., Magnetoimplosive Generators, Soviet Physics - Uspekhi, Vol. 9, No. 2, pp 294-299, (in English translation), Sept. - Oct. 1966.

12. Fowler, C.M., Megagauss Physics, Science, Vol. 180, No. 4083, pages 261-267, April 20, 1973.

SYMBOLS USED

A	Area (m^2)
B	Flux density (Wb/m^2)
d, D	Diameters (m)
E	Electric field intensity (V/m)
f	Subscript referring to final state of a system
I	Current (A)
K	Sheet surface current (A/m)
L	Inductance (H)
ℓ	Length dimension of cylinder (m)
$\underline{n}$	Vector of unit length normal to a surface
o	Subscript referring to initial state of a system
p	Pressure
t	Time (s)
W	Energy (J)
δ	Skin depth (m)
ϕ	Flux (Wb)
σ	Conductivity (mho/m)
μ_o	Permeability of vacuum ($4\pi \times 10^{-7}$ H/m)
τ	Time constant of exponential fold increase (s)

III. C. Electronic Modulators as High Power Video Pulse Sources

During World War II, the need arose to develop equipment to pulse the magnetron microwave generators in military radars [1]. As a result, techniques for designing these modulators are now well-understood and well-developed.

In September 1973, the 11th modulator symposium [2] was held. Technical papers presented new designs, gave details of new devices, described how recent technological advances could be incorporated into modulators, and discussed new modulator applications.

One may ask: how far does the state-of-the-art of modulator design permit one to go in generating large pulses? An exceptionally interesting paper by D. L. Pruitt [3] of RCA addressed this question.

His first conclusion was that the most sensible choice was the line-type modulator with hydrogen thyratron switching. In principle, a line-type pulser consists of a high-voltage power supply in combination with a resonant charging inductor; these serve to store energy in a pulse-forming-network (PFN). If designed properly, nearly twice the power supply voltage (V in Fig. 1 below) appears across the capacitors of the PFN. Switch S is then closed, causing a pulse of amplitude V and duration $2\sqrt{L_{tot}C_{tot}}$ to appear across terminals a-b when the resistance $r = Z_o$. Generally, the characteristic impedance $Z_o = \sqrt{\frac{L}{C}}$ of the PFN is much smaller than the actual load resistance R. For this reason, a pulse transformer is needed to accomplish matching.

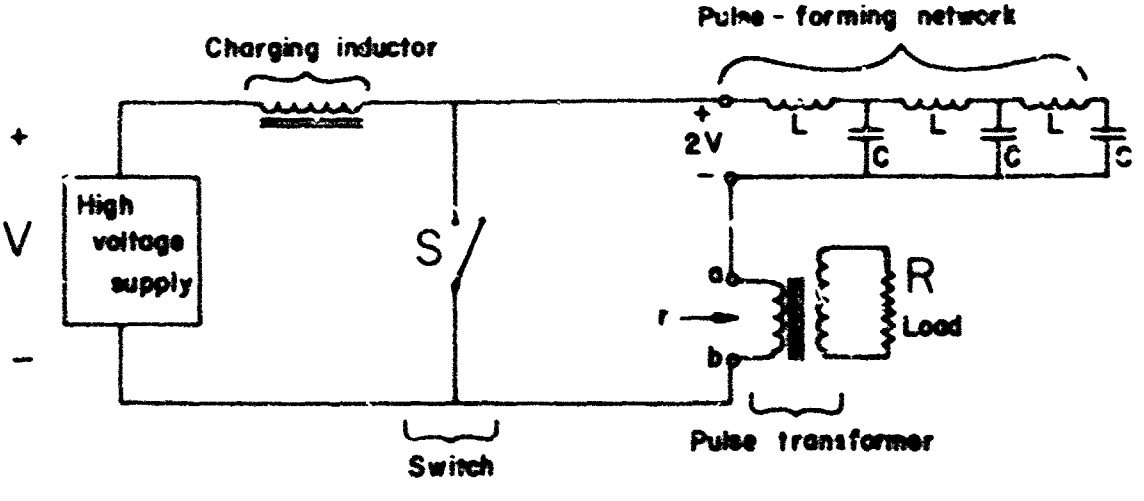

A Basic Line-Type Modulator

Switching is most often done using hydrogen thyratrons. When S is in the open position, it must withstand twice the power supply voltage, and in the closed (fired) position, it must pass very large currents. At present, these tubes have maximum ratings up to 160kV (English Electric CX1193) and 10kA peak (Tung-Sol CH1222).

Using state-of-the-art components, Pruitt proposed a design for a super-power modulator. The set of specifications listed below was shown to be achievable, but at the price of using 60 KU-275 ITT thyratrons, and 12' x 20' x 50' space to house all the equipment.

An Achievable Super-Power Modulator Design [3]

Peak power	2.5 GW	Average power	10 MW
Pulse width	20μsec	Load voltage	200 kV (peak)
Pulse rise time	5μsec (max)	Load current	12.5 kA (peak)
		Repetition rate	200 pps
		Continuous duty	

It is reasonable to accept this result as the limit of what is attainable with present-day modulator techniques.

REFERENCES

1. G. N. Glasoe and J. V. Lebacqz, "Pulse Generators," McGraw-Hill, 1948.

2. Conference Record, 11th Modulator Symposium held Sept. 18, 19, 1973 in Belmont Hotel, New York, N.Y., IEEE-AGED (Advisory Group on Electron Devices), IEEE Number 73, CHO 773-2 Ed.

3. D. L. Pruitt, "Design Considerations for Super Power Pulse Modulators," pages 106-112 in Conference Record.

Symbols Used

C	capacitance (F)
L	inductance (H)
r, R	resistance (Ω)
S	switch
V	voltage (V)
Z_o	characteristic impedance (Ω)

III. D. Video Pulse Generation using Relativistic Electron Beams

One way to make high power video pulses is by utilizing very high voltages to create high current discharges. At the present time, such discharges are of great interest because of their possible application to controlled nuclear fusion [1], and because they may be used to produce high-power microwave pulses [2, 3, 4, 5].

The achievement of temperatures and densities high enough for fusion has for many years been approached through the avenue of magnetic confinement of plasmas; more recently, via illumination of deuterium-tritium pellets with intense laser beams; and most recently via pellet bombardment with very high energy, extremely dense pulsed electron beams [6]. Generation of these beams is the subject of this section of the report. For fusion purposes, it is of prime interest to obtain high power densities. An appreciation of the order of magnitude of the accompanying video pulse parameters may be gained from Table I below, which lists some electron beam machines. Availability of these high voltage generating units may be partly a result of military EMP simulation studies [1, 7].

Relativistic beams have also been used to produce 30 nanosecond - 10 MW bursts of microwave power in the range 7.8-9.7 GHz by coupling to rigid slow wave structures [2]. More recently, microwave bursts have been obtained by coupling to rippled magnetic fields [3, 4, 5], with X-band output pulses as high as 1 GW [5].

Megavolts for making pulses are obtained from: a Van de Graaff generator; a Marx circuit; [8] a Blumlein line [8]. The Marx circuit (see Fig. 1) stores energy by first charging many capacitors in parallel; then, it switches them to a series connection. The Blumlein line uses a transmission line to double an available power supply voltage for a short pulse interval.

Table I - Electron Beam Machines

Device Name	Location	V(MV)	I(MA)	τ(n sec)	P(TW)	E(MJ)	Informat. Source	
Aurora	Harry Diamond Labs, MD.	12	1.7	125	20	2.5-3	Lubkin	(1)
FX-75	Boeing Radiation Effects Lab	3.5-5	.040	30	.14-	.0042-	Morrow, et al	(11)
FX-25	AF Weapons Lab, NM	2.5-3	.025	40	.07	.001	Lubkin	(1)
Nereus	Sandia	.2	.1	30	.02	.0006	Yonas, et al	(14)
Slim		.25	.25	100	.06	.00		
Hydra	Sandia	1	1	80	1	.08	Lubkin	(1)
—	Physics	10	.3	?	3	?	Ford, et al.	(15)
—	International	3	.05	30	.15	.0045	Link	(10)
—	Livermore	6	.05	30	.3	.009	Lubkin	(1)
Gamble I	NRL	.75	.5	80+	.4	> .03	Lubkin	(1)
Gamble II	Wash., DC	~ 2	~1.5	?	<3?	< .2		
—	USSR	< 3	< .1	—	<.3	—	Lubkin	(1)

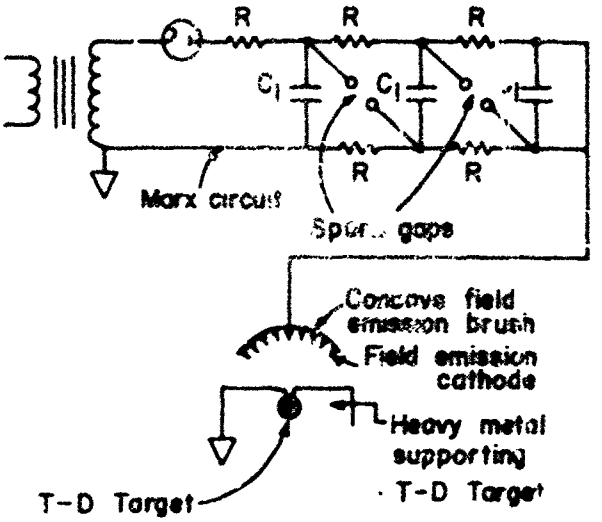

Fig. 1 illustrating [6]:

a) Marx Circuit

b) Idea underlying current interest in high energy, tightly confined pulsed electron beam for CTR

Initially, single point cathodes were employed to create ~3 MV pulsed discharges. Direct field emission gave currents of the order of 50 kA. Observations of the discharge current beam [9, 10] indicated that the behavior in the post-anode drift region was controlled by magnetic fields generated by the current stream itself. In general, divergence of a dense electron beam is to be expected. However, partial neutralization of the beam by positive ions reduces the diverging Coulomb force sufficiently compared to the converging magnetic force to permit the beam to become self-pinching.

A large step forward in the generation, confinement and guidance of high energy beams was described by Morrow, et al. [11] reporting the work of a group under W. H. Bennett. They found that a small-diameter glass rod could be used to guide the stream, and to serve as a cathode. In addition, the degree of current concentration was greater than had previously been achieved, a result subsequently confirmed by Condit and Pellinen [12, 13]. Crucial experiments [11] are illustrated in the sketch below. From these and additional experiments, it was concluded that the partially neutralized electron beam (~0.2 MA) was pinched against the glass guide, and that the tip of the glass rod was the effective cathode.

Whether there is an upper limit to the size of the total current pulse is not clear from the work done so far. Of course, an upper limit to the total pulse energy is set by the energy stored in the high voltage generating unit.

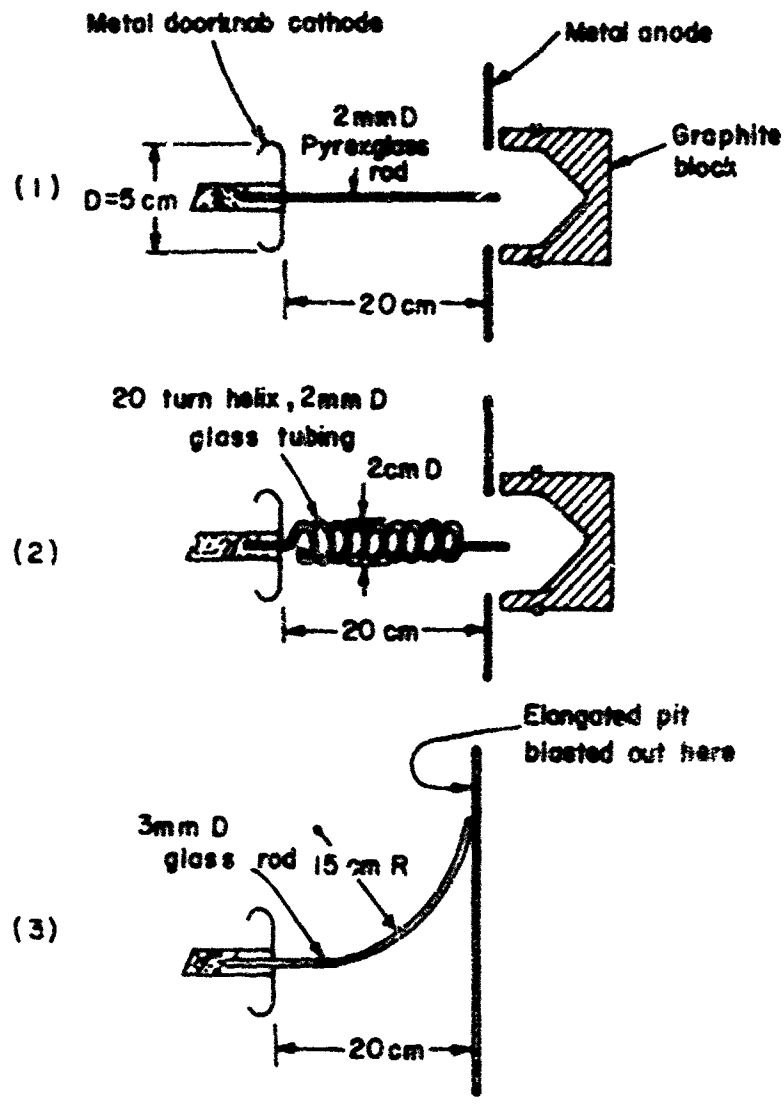

Fig. 2 Three important experiments [11] illustrating guidance of partially neutralized electron beam discharge by glass rods. Faraday cup current measuring assembly not shown. Approximate discharge conditions: 30 n sec, 3.5 MV, >.2 MA, 10^{-4} Torr.

References

1. G. B. Lubkin, "Many Laboratories Try for Fusion with Electron Beams," Physics Today, April 1973, pages 17-20.

2. J. A. Nation, "On the coupling of an high-current relativistic electron beam to a slow wave structure," Applied Physics Letters, Vol. 17, No. 11, Dec. 1, 1970, pages 491-494.

3. M. Friedman and M. Herndon, "Emission of coherent microwave radiation from a relativistic electron beam propagating in a spatially modulated field," Physical Review Letters, Vol. 29, No. 1, July 3, 1972, pages 55-58.

4. W. M. Manheimer and E. Ott, "Theory of Microwave generation by an intense relativistic electron beam in a rippled magnetic field," Naval Research Laboratory, Memorandum Report 2588, May 1973.

5. V. L. Granatstein, M. Herndon, Y. Carmel and J. A. Nation, "Gigawatt Microwave Emission from a Highly Relativistic Intense Electron Beam," Bulletin of the American Physical Society, Series II, Vol. 18, No. 10, October 1973, pages 1354-1355.

6. F. Winterberg, "The Possibility of Producing a Dense Thermonuclear Plasma by an Intense Field Emission Discharge," Physical Review, 5 October 1968, Vol. 174, No. 1, pages 212-220.

7. Proceedings of the Technical Coordination Conference on EMP Biological Effects, July 1970, Albuquerque, N. M., Sponsored by Lovelace Foundation.

8. G. N. Glasoe and J. V. Lebacqz, "Pulse Generators," McGraw-Hill, 1948, pages 494-496; 463-468.

9. S. E. Graybill and S. V. Nablo, "Observations of Magnetically Self-Focusing Electron Streams," Applied Physics Letters, Vol. 8, No. 1, 1 January 1966, pages 18-20.

10. W. T. Link, "Electron Beams from 10^{11} - 10^{12} Watt Pulsed Accelerators," IEEE Trans. on Nuclear Science, Vol. NS-14 No. 3, June 1967, pages 777-781.

11. D. L. Morrow, J. D. Phillips, R. M. Stringfield, Jr., W. O. Doggett and W. H. Bennett, "Concentration and Guidance of Intense Relativistic Electron Beams," Applied Physics Letter, Vol. 19, No. 10, 15 Nov. 1971, pages 441-443.

12. W.C. Condit, Jr. and D. Pellinen, "Impedance and Spot-size Measurements on an Intense Relativistic-Electron-Beam Device," Physical Review Letters, Vol. 29, No. 5, 31 July 1972, Pages 263-265.

13. W.C. Condit, Jr., D.O. Trimble, G.A. Metzger, D.G. Pellinen, S. Heurlin and P. Creely, "Generation and Diagnosis of Terawatt/Centimeter^2 Electron Beams," Physical Review Letters, Vol. 30, No. 4, 22 January 1973, pages 123-125.

14. G. Yonas, K.R. Prestwich, J.W. Poukey and J.R. Freeman, "Electron Beam Focusing Using Current-Carrying Plasmas in High ν/γ Diodes," Physical Review Letters, Vol. 30, No. 5, 29 January 1973, pages 164-167.

15. F.C. Ford, D. Martin, D. Sloan and W. Link, "10^{12} W Pulsed Accelerators," Bulletin of the American Physical Society, Vol. 12, 1967, page 961 (Abstract only).

IV. R.F Pulse Generation: High Power Bursts of Microwave Radiation

A. Microwave Pulse Generation using Relativistic Electron Beams

Recently, high power microwave pulses have been generated by conversion of part of the energy in relativistic electron beams into microwaves.

a) At Cornell, Nation [1] used an annular electron beam to couple to a slow wave structure, as shown in Fig. 1. The beam and microwave pulse characteristics are tabulated below:

Beam Pulse		Microwave Pulse	
Max. Voltage	500 kV	Power	10 MW
Max. Current	40 kA	Duration	30 n sec.
Max. Power	2.0 GW	Frequency	7.8-9.7 GHz
Outer (inner) beam radius	3.4(3.0) cm.		
Duration	60 n sec.		

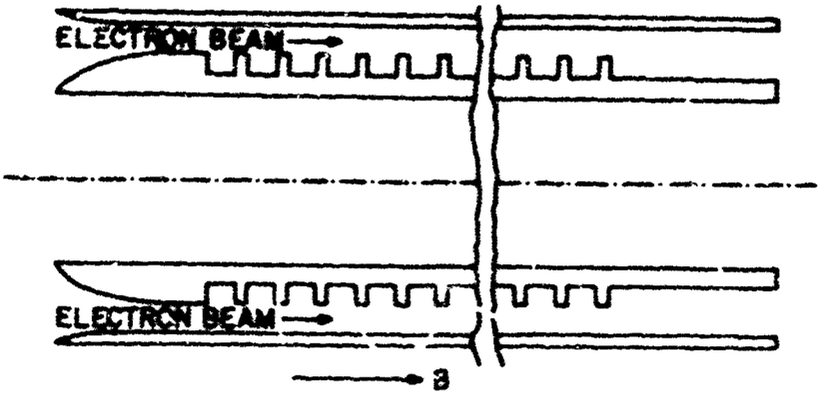

Fig. 1. Slow-Wave Structure for Microwave Pulse Generation

The frequency depended upon the electron injection energy. Power was greatest near electron cyclotron frequency. Pressure was approximately 2×10^{-4} Torr. The longitudinal magnetic field B shown in Fig. 1 was needed to hold the beam together. Conversion efficiency was about (10 MW/2 GW) = .05%.

b) At NRL, Friedman and Herndon [2, 3] used a rippled magnetic field with pressures near 0.5×10^{-4} Torr (see Fig. 2) to induce a beam to generate microwave pulses in circular waveguide. Most of the power was in the X-band range 6.5-12 GHz, although there was also harmonic generation 10 dB below this level. Wavelength was $\propto$ to the spatial period of B. They used an annular electron beam with characteristics:

Voltage	700 kV
Current	18 kA
Power	1.3 GW
Beam Radius	1.7 cm
Duration	50 n sec

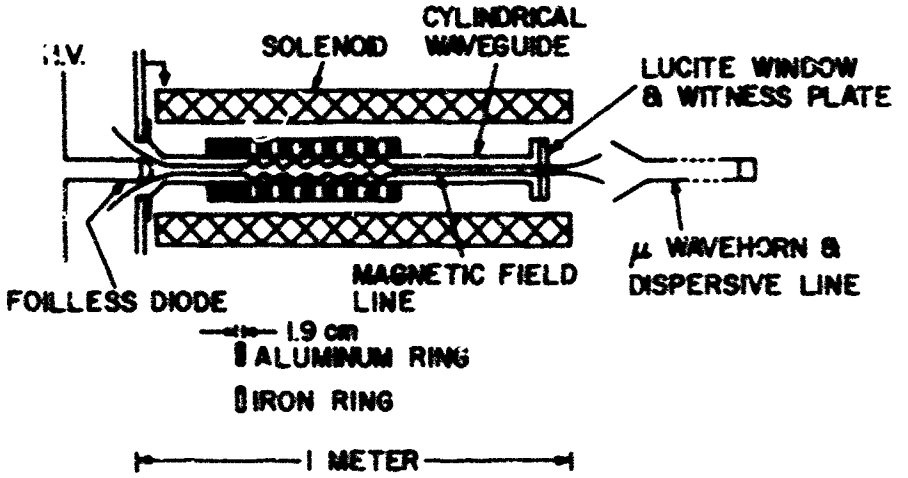

Fig. 2. Rippled Magnetic Field Arrangement for Microwave Pulse Generation

Manheimer and Ott [4] discussed this method of pulse generation from a theoretical point of view.

c) Subsequently, these two groups collaborated, and reported [5] the results of using a larger beam machine (3.3 MV, 80 kA) with the rippled magnetic field arrangement. They were able to obtain output pulses in the X-band as high as 1 GW.

References

1. J.A. Nation "On the coupling of an high-current relativistic electron beam to a slow wave structure" Applied Physics Letters Vol 17 No. 11, Dec. 1, 1970, pp. 491-494.

2. M. Friedman and M. Herndon "Microwave emission produced by the interaction of an intense relativistic electron beam with a spatially modulated magnetic field" Physical Review Letters Vol 28 No. 4, Jan. 24, 1972, pp. 210-212.

3. M. Friedman and M. Herndon "Emission of coherent microwave radiation from a relativistic electron beam propagating in a spatially modulated field" Physical Review Letters Vol 29 No. 1, July 3, 1972, pp. 55-58.

4. W.M. Manheimer and E. Ott "Theory of microwave generation by an intense relativistic beam in a rippled magnetic field" Naval Research Laboratory Memorandum Report 2588, May 1973.

5. V.L. Granatstein, M. Herndon, Y. Carmel and J.A. Nation "Gigawatt microwave emission from a highly relativistic intense electron beam" Bulletin of the American Physical Society Series II Vol 18 No. 10, Oct. 1973, pp. 1354-1355.

IV. B. Radiating Plasmas

1. Introduction

Considerable progress has recently been made in obtaining high power bursts of electromagnetic radiation from plasmas. Cowan and Freeman [1], used as a radiation source an arc in a deuterium plasma. They were able by this means to achieve a black body radiation spectrum with peak powers in the order of terawatts and energies in the order of megajoules. A great step forward could be achieved if the high powers which plasmas are capable of producing could be channeled into the line spectra which rigid structures can yield. With this thought in mind, we consider here those processes in plasmas which give rise to monochromatic radiation.

The radiation spectra emitted by plasmas at radio and microwave frequencies can be grouped as follows:

a. Spectra that can be interpreted on the basis of the classical theory of thermal radiation. The radiation originates from the motions of Maxwellian electrons (bremsstrahlung, and cyclotron radiation). Its intensity cannot exceed that of a black body with temperature equal to that of the free electrons. This is the radiation obtained by Cowan and Freeman in their "flash lamp."

b. Nonthermal spectra arising from the noncooperative motions of non-Maxwellian electrons. Departures from the Maxwellian velocity distribution stem from electrical currents, beam injection, or selective loss of particles (loss cone).

c. Radiation originating from cooperative motions of the free charges induced by perturbation of the plasma (plasma modes). When driven from non-Maxwellian electron distribution, such perturbations can reach high intensity levels. This mechanism, which is of particular interest for the generation of high power bursts of radiation, is similar to that operative in microwave tubes with the plasma replacing the slow wave structure.

Plasmas can develop a great variety of unstable modes. High gains have been observed in longitudinal waves propagating along, or in the absence of, a static magnetic field B_o [2]. Unfortunately two reasons militate against the practical utilization of these modes: (a) Onset of nonlinear effects with consequent saturation of the wave at relatively low levels of intensity [3]. (b) Inefficient coupling of the longitudinal waves to radiating modes. Transverse modes propagating in nonmagnetized plasmas are characterized by low gains.

For these reasons, and because a magnetic field always exists in the presence of the large currents required to generate large amounts of power, the investigation was centered on transverse waves propagating in magneto plasmas. Stix [3] has shown that in this case saturation occurs at much higher intensities. Instabilities occur in the neighborhood of the cyclotron frequency $f_c = \frac{e B_o}{2 \pi m}$ and its harmonics. Since for cyclotron radiation in

the microwave range would require very high magnetic fields, only instabilities involving electron motions were considered. The ions, then, simply serve to provide a neutralizing positive background.

2. Radiation in Ramsauer gases

The Ramsauer effect provides a mechanism for the generation of non-thermal spectra in the absence of collective phenomena (class 2). As was reported by Wachtel and Hirschfield [4] and by Terumichi et al. [5], the negative absorption or amplification of a transverse wave at cyclotron frequency by argon, krypton and xenon occurs in the range where the collision frequency increases rapidly with the electron energy. The electrons traveling with velocity $v_{\parallel}$, such that the resonant condition

$$\omega - k_{\parallel} v_{\parallel} = n \omega_c$$

is satisfied, interact strongly with the wave. The direction of the energy transfer depends on the phase with which they "sense" the wave. Those electrons which are accelerated are more likely to collide and be thrown out of phase than those which are decelerated and give energy to the wave. On the average, then, the electrons causing wave growth are allowed to interact with the wave for a longer period of time and their effect predominates. This mechanism has also been studied by Tanaka and Mitani [6] and Field et al [7]. It is not expected to lead to powerful radiation sources, because the energy of the interacting electrons is relatively low (< 4 ev).

3. Anistropy Instabilities

According to Vedenov [8] a homogeneous plasma having a velocity distribution which is anisotropic with respect to B_o will be unstable when

$$\frac{T_{\perp}}{T_{\parallel}} + \frac{\omega_c}{\omega} \left(1 - \frac{T_{\perp}}{T_{\parallel}}\right) < 0.$$

Sagdeev and Shafranov [9] showed that an electron plasma can support only the right circularly polarized wave ($\omega > o$) and hence be unstable only when $T < T_{\parallel}$ and

$$o < \omega < \left(1 - \frac{T_{\parallel}}{T_{\perp}}\right) \omega_c .$$

This instability has been observed in experiments conducted by Gitomer and Sohet [10] and Ikegami et al [11]. The latter obtained 10W at the fundamental frequency of 2.1 GHz and powers decreasing in the ratio of 10dB in the successive harmonics.

4. Synchrotron Radiation

The collision frequency between the electrons and ions decreases rapidly with increasing electron energy. When electrons are accelerated by an electric field, a condition may be reached in which the dynamical friction

is inadequate to balance the electric field and a group of electrons "runs away" and can easily acquire relativistic velocities. Since a relativistic electron radiates most of its radiation in the direction of its motion, an observer will detect a radiation spectrum consisting of harmonics of the cyclotron radiation.

Instabilities leading to synchrotron radiation were predicted by Zheleznyakov and Suvorov [12], and by Schneider, and observed by Bott [13] and by Hirshfield and Wachtel [14]. The observed powers did not exceed 1 W. Blanken and Kuckes [15] give a physical explanation for the instability they had observed. They claim that the relativistic variation of the cyclotron frequency with energy causes a coherent phase ordering of the electrons in the field of the wave. This theory was further elaborated by Blanken, Stix, and Kuckes [16] who observed saturation of the emission at 50 dB above the synchrotron level (10-100 ev).

5. Cold beams parallel to B_o

The presence of a cold electron beam traveling parallel to B_o can cause a plasma instability which, according to Stix [3], occurs when $v_{\parallel} = \frac{\omega \pm \omega_c}{k}$. Two modes are possible depending on the sign of $v_{\parallel}$. In both modes the fields rotate in the opposite sense of the electrons they are interacting with and $|\omega| < |k v_{\parallel}|$.

There seems to be no experimental verification of this instability.

6. Diocotron Instability

An electron beam propagating perpendicular to crossed E and B fields may excite a plasma instability similar to the mode which is operative in magnetrons. [17-19]. Growth results from the fact that in a magnetic field the acceleration is perpendicular to the direction of the electric field. The instability has been observed in reflex discharges [20].

7. Parametric Interactions

Experiments aimed at achieving thermonuclear fusion temperatures, by means of electron cyclotron resonance heating, have demonstrated the existence of a variety of parametric interactions involving more than two plasma modes. The possibility of microwave generation has been studied by Stone, Serafim, and Levi [21].

The driving mechanism consists of either an ac electric field impressed transversely to the applied magnetic field, or bunches of particles injected with preferential phase. With wave propagating along B_o, six absolute instabilities are found to result from the coupling between two electronic plasma modes, and three more result from the coupling between an electronic mode and an ion cyclotron branch. Since the growth rates are proportional to $v_{\perp}/c$, or $(v_{\perp}/c)^2$, these instabilities may yield large powers with relativistic beams.

Under certain symmetry conditions the infinite cascade of coupled frequencies, that usually occurs in parametric problems, is limited to three. Such a truncation of the cascade cannot be attained in the case of waves propagating across B_o [22].

References

1. M. Cowan and J.R. Freeman, J. Appl. Phys. 44, 1595-1603 (1973).
2. F.W. Crawford, Proc. IEEE, 59, 4-19 (1971).
3. T.H. Stix, The Theory of Plasma Waves, McGraw-Hill 1962.
4. J.M. Wachtel, and J.L. Hirschfield, Phys. Rev. Lett. 19, 293-5, 1967.
5. Y. Terumichi, T. Idehara, I. Takahashi, H. Kubo, and K. Mitani, J. Phys. Soc. of Japan 20, 1705-1710, (1965).
6. S. Tanaka, and K. Mitani, J. Phys. Soc. of Japan 19, 1376 (1964).
7. H. Fields, G. Bekefi, and S.C. Brown, Phys. Rev. 129, 507-515 (1963).
8. A.A. Vedenov, Theory of Turbulent Plasmas, Israel Inst. for Scientific Translations, Jerusalem (1966).
9. R.Z. Zagdeev and V.D. Shafranov, Sov. Phys. JETP 12, 130 (1961).
10. S.J. Gitomer and J.L. Sohet, Phys. Fluids 13, 413 (1970).
11. H. Ikegami, H. Ikezi, M. Hosokawa, T. Takayama, and S. Tanaka, Phys. Fluids, 11, 1061-3 (1968).
12. V.V. Zheleznyakov, and E.V. Suvorov, Sov. Phys. JETP 27, 335 (1968).
13. J.B. Bott, Phys. Lett. 14, 293-4, (1965).
14. J.L. Hirshfield and J.M. Wachtel, Phys. Rev. Lett. 12, 533-6, (1964).
15. R.A. Blanken and A.F. Kuckes, Plasma Phys. 11, 321-31 (1969).
16. R.A. Blanken, T.H. Stix, and A.F. Kuckes, Plasma Phys. 11, 945-59, (1969).
17. O. Buneman, Nature, 165, 474 (1950).
18. G.G. MacFarlane and M.C. Hay, Proc. Phys. Soc. (London) 63B, 409 (1950).
19. R.G.E. Hutter, Beam and Wave Electronics in Microwave Tubes, Van Nostrand, Princeton (1960).
20. W.A. Knauer, A. Fafarman, and R.L. Poeschel, App. Phys. Lett. 3, 111 (1963).

References (continued)

21. F.T. Stone, P.E. Serafim, and E. Levi, Phys. Fluids 16, 921-8 (1973).

22. F.T. Stone "Parametric Interactions in Plasmas," Ph.D. (EE) Dissertation P.I.B. June 1970.

Symbols Used

B_o	(static) magnetic flux density	($Wb/m^2 = T$)
c	velocity of light in vacuum	(2.998×10^8 m/s)
e	charge on an electron	(1.602×10^{-19} C)
f	frequency of wave incident on plasma	(Hz)
f_c	electron cyclotron frequency	(Hz)
k	wavenumber (2π/wavelength)	(m^{-1})
$k_{\parallel}$	wavenumber parallel to B_o	(m^{-1})
m	mass of an electron	(9.11×10^{-31} kg)
n	an integer	
$T_{\parallel}$; $T_{\perp}$	electron temperature parallel; perpendicular to B_o	(^oK)
$v_{\parallel}$; $v_{\perp}$	velocity parallel; perpendicular to B_o	(m /s)

ω; ω_c $\quad 2\pi f$; $2\pi f_c$

IV. C. Rapid Release of Stored Microwave Energy

We wish to consider the possibility of microwave pulse generation by rapid energy release from a cavity. To gain insight into this question, pulse generation by Q-switched lasers is first discussed.

At optical wavelengths, giant pulses of 5-50 n sec duration can be generated by Q-switching [1]. In principle, this is accomplished in the following way: An optical cavity containing a medium capable of lasing is terminated with reflecting mirrors at the ends. The atoms are pumped into their high energy state by some means, but lasing action is suppressed by deliberately interposing a shutter between one of the mirrors and the cavity proper, or by deliberately making the cavity lossy. After substantially complete population inversion has been achieved, the loss mechanism is suddenly removed, lasing action takes place, and the entire excited population suddenly drops to its lower state. Pulse energy is less than $h\nu n$, where n is the number of excited atoms in the cavity. Rotating mirrors and bleachable dyes have been used to switch the cavity from the lossy to the lossless state.

The diagram below is intended to clarify the description. When the population inversion is sufficiently great, the spontaneous emission and the stimulated emission become large enough to switch the dye from its absorbent to its transparent state.

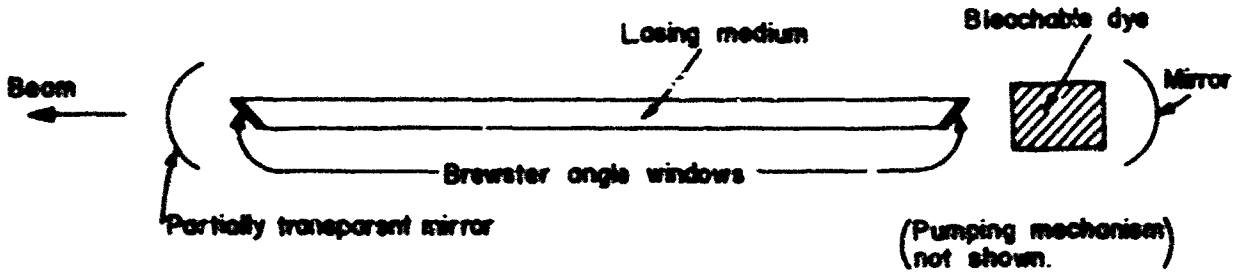

Fig. 1. Principle of a Q-Switched Laser

We wish to center attention on this aspect of Q-switching: the storage of energy within a cavity, followed by its sudden triggered release. Is it possible to do something similar with microwaves?

Suppose a microwave cavity consisting of a length of waveguide short-circuited at the ends is filled with energy. The diagram does not show the primary energy source (a pulsed magnetron, perhaps) or the means by which

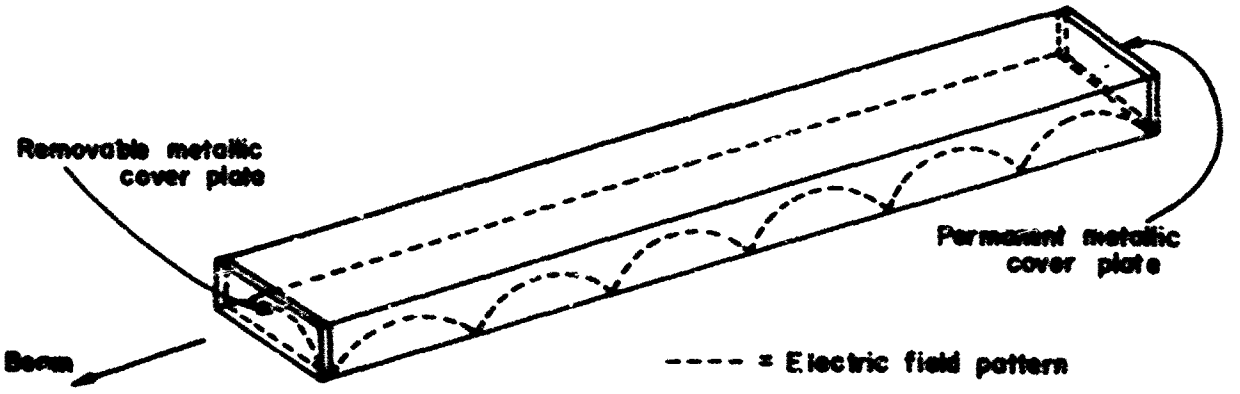

Fig. 2. TE_{10} Microwave Cavity

this energy is coupled into the cavity. It is assumed that the energy content (W, Joules) is limited by the maximum permissible electric field strength (E_{max}, V/m). We now wish to relate these two quantities.

For a plane wave in empty space, the instantaneous local energy density is

$$\mathcal{E}(t) = \tfrac{1}{2}\epsilon_o E^2 + \tfrac{1}{2} u_o H^2 \ J/m^3. \quad \text{Since } \frac{E}{H} = \sqrt{\frac{\mu_o}{\epsilon_o}}$$

$$\mathcal{E}(t) = \epsilon_o E^2.$$

In terms of the maximum value of the (sinusoidally varying) incident electric field E_{inc}, the time average energy density is

$$\mathcal{E}_1 = \tfrac{1}{2}\epsilon_o E^2_{inc}.$$

Next, we assume reflections are created by a metallic plate normal to the propagation direction. A standing wave exists, so that the electric field now varies in amplitude from 0 to 2 E_{inc}. When the energy density is now averaged over distances that are multiples of a wavelength, the time and space averaged energy density for total reflection is double that for the incident wave only; that is, the energy density is now

$$\mathcal{E}_{AV} = \epsilon_o E^2_{inc} \ J/m^3.$$

In terms of the maximum instantaneous electric field $E_{max} = 2\ E_{inc}$,

$$\mathcal{E}_{AV} = \tfrac{1}{4}\epsilon_o E^2_{max} \ J/m^3.$$

Next, we assume for simplicity that the same situation prevails inside the microwave cavity, except for a factor of $\frac{1}{2}$ due to the transverse

sinusoidal field variation. Hence we have

$$W = \tfrac{1}{2}\,(\tfrac{1}{4}\,\epsilon_o\,E^2_{max})\times(\text{Cavity Volume})\ \text{Joules}$$

For a numerical estimate, assume standard S-band (3 GHz) waveguide with $1\tfrac{1}{2}$" x 3" outer cross-sectional dimensions, .080" wall thickness, 2 meter length, 3000 kV/m breakdown - limited maximum electric field:

$$W = \tfrac{1}{2}\,(\tfrac{1}{4}\times 8.85\times 10^{-12}\ \text{F/m})\times(3\times 10^{6}\ \text{V/m})^2\ (2\times .034\times .068) = .046\ \text{J}.$$

Pulse width τ is nearly the time for the wave to travel 2 guide lengths to achieve complete emptying of the cavity:

$$\tau \approx \frac{2\,l}{c} = \frac{4\text{m}}{3\times 10^{8}\ \text{m/s}} = 13\ \text{n sec}$$

Associated bandwidth is $BW \approx \frac{2}{\tau} = \frac{2}{13}\ \text{GHz} = 0.15\ \text{GHz}.$

Evidently, the cavity energy content is quite low. However, the guide cross-section is pessimistically low. One may easily visualize a length of waveguide with cross-sectional area 2 orders of magnitude greater. This would yield a stored energy 100 times greater, and a peak power 100 times greater $(100\times\frac{.046}{13\times 10^{-9}} = 350\ \text{MW})$. Mode control measures would have to be used, however. Also, increases in length by orders of magnitude are easily achievable, but this simultaneously increases the pulse width by the same factor without increasing the peak power.

The engineering realization of such a device was considered by J. W. E. Griemsmann [2, 3], who made detailed calculations and offered sample designs. The microwave cavity, instead of being a linear one, was visualized as a ring [4] structure fed by a directional coupler from an auxiliary waveguide. After energy storage within the ring was complete, a controlled microwave switch (see, for example, refs. (5), (6)) served to divert the stored energy into an output waveguide, thus into a horn of rectangular aperture, then into space. Since the basic limitation was the same as that discussed earlier (breakdown), "oversize" or multi-mode rectangular waveguide with appropriate mode control techniques was utilized.

In conclusion, the idea of rapid release of stored microwave energy is interesting, but requires as a prime power source an auxiliary generator of microwave power (magnetron, for example) for its implementation. In addition, a considerable amount of engineering development would be required.

References

1. W. V. Smith and P. P. Sorokin "The Laser" Mc-Graw-Hill 1966 pages 147 ff.

2. J. W. E. Griemsmann "Preliminary Design Considerations of a Microwave Flywheel" Polytechnic Institute of Brooklyn report number R-722-59, PIB-650, Memorandum 21, 5 March 1959, AFOSR contract AF-18 (600)-1505.

3. J. W. E. Griemsmann "Design Considerations for a Microwave Flywheel" Polytechnic Inst. of Bklyn. Report R-452.15-59, Quarterly Progress Report 15, 15 Jan '59-14 Apr '59, JSTAC, contract AF-18(600)-1505, pages 45-50.

4. L. J. Milosevic and R. Vautey "Traveling-Wave Resonators" IRE Trans. on MTT, Vol. MTT-6 No. 2, Apr 1958, pages 136-143.

5. H. Goldie "Fast, High-Power, C-band Microwave Switch" Polytechnic Inst. of Bklyn. Report R-452.22-62 Progress Report 22, 1 Apr '62-30 Sept 1962, JSTAC, Grant AF-AFOSR-62-295 pages 83-93, supported by RADC contract AF-30(602)-2135.

6. M. Sucher "DC Triggered Microwave Spark Gap Switch" Polytechnic Inst. of Bklyn Report R-452.23-63 Progress Report 23, 1 Oct 1962-31 March 1963, JSTAC Grant AF-AFOSR-62-295, pages 69-74. Work supported by RADC contract AF-30(602)-2135.

Symbols Used

c	velocity of light in vacuum (2.998×10^8 m/s)
E	instantaneous electric field strength (V/m)
E_{inc}	maximum value of E in incident wave
E_{max}	value of E just causing breakdown
$\mathcal{E}(t)$	instantaneous local energy density (J/m^3)
$\mathcal{E}_1$	time average energy density (J/m^3)
$\mathcal{E}_{AV}$	time and space averaged energy density (J/m^3)
H	instantaneous magnetic field strength (A/m)
ℓ	length (of a linear cavity) (m)
W	energy (content of a cavity) (J)
μ_o	magnetic permeability of vacuum ($4\pi \times 10^{-7}$ H/m)
ϵ_o	electric permittivity of vacuum (8.85×10^{-12} F/m)
τ	width of microwave pulse (s)

V. Parametric Studies of Pulse Generation

A. Introduction

All known types of electrical power converters can be successfully employed for pulse generation. It is therefore interesting to determine which type is best for a particular application. Rioux was able to characterize power converters by a set of intelligently selected parameters, and used this as the basis for formulating and investigating the problem. The following discussion is based on his work [1,2].

We restrict ourselves to converters of the magnetic type in which the conversion process can be associated with a force density (force per unit volume).

$$\underline{f} = \underline{J} \times \underline{B} - \tfrac{1}{2} (\underline{\nabla} \mu) H^2 \qquad (1)$$

where

$\underline{J}$ = electric current density (A/m^2)

$\underline{B}$ = magnetic flux density (Wb/m^2)

μ = magnetic permeability (assumed isotropic) (H/m)

$\underline{H}$ = magnetic field intensity (A/m)

The total force F applied to a rigid body is obtained by performing an integration over the whole volume V. We consider here two structures in relative motion, the field and the armature. For either structure,

$$\underline{F} = \int_V (\underline{J} \times \underline{B} - \tfrac{1}{2} (\underline{\nabla} \mu) H^2) \, d V \qquad (2)$$

For the purpose of classification of the various converter types, it is desirable to introduce the Maxwell stress tensor and to convert this volume integral into an integral over a suitable surface S bounding V.

To this end we make use of Maxwell's equations in the quasistatic approximation

$$\underline{\nabla} \times \underline{H} = \underline{J} \text{ and } \underline{\nabla} \cdot \underline{B} = 0, \qquad (3)$$

and of the vector identity

$$\begin{aligned} \underline{\nabla} (\underline{B} \cdot \underline{H}) &= \underline{\nabla} (\mu \underline{H} \cdot \underline{H}) = (\underline{\nabla} \mu) H^2 + \mu \underline{\nabla} (\underline{H} \cdot \underline{H}) \\ &= (\underline{\nabla} \mu) H^2 + 2\mu [\underline{H} \times (\underline{\nabla} \times \underline{H}) + (\underline{H} \cdot \underline{\nabla}) \underline{H}], \end{aligned} \qquad (4)$$

to obtain

$$F = \int_s [\mu \underline{H} (\underline{H} \cdot \underline{n}) - \frac{\mu}{2} H^2 \underline{n}] \, ds \qquad (5)$$

where $\underline{n}$ = normal unit vector.

To evaluate $\underline{F}$, the total force acting on the structure, the bounding surface must be chosen outside the magnetic material, so that $\mu = \mu_o$ and $\underline{H} = \underline{H}_o$.

The field intensity $\underline{H}_o$ can be expressed in terms of the magnetic field prevailing inside the magnetic material by imposing the condition of continuity of the normal component of $\underline{B}$ and tangential component of $\underline{H}$ across the discontinuity. The result is

$$\underline{H}_o = \underline{H} + [(\frac{\underline{B}}{\mu_o} - \underline{H}) \cdot \underline{n}] \cdot \underline{n} \qquad (6)$$

When the magnetic polarization vector $\underline{M}$ is introduced, the result may be rewritten:

$$\underline{H}_o = \underline{H} + (\underline{M} \cdot \underline{n}) \underline{n} \qquad (7)$$

Finally substituting μ_o for μ and $\underline{H}_o$ for $\underline{H}$, in Eq. (5) and making use of Eq. (7) we obtain:

$$F = \int \mu_o [\underline{H} (\underline{H} \cdot \underline{n}) - \tfrac{1}{2} H^2 \underline{n} + (\underline{M} \cdot \underline{n}) \underline{H} + \tfrac{1}{2} (\underline{M} \cdot \underline{n})^2 \underline{n}] \, ds \qquad (8)$$

On the basis of this equation Rioux defines the following classes of converters:

Class 1: Air-cored machines in which $\underline{M} = o$. The force is contributed by the term $\underline{H} (\underline{H} \cdot \underline{n}) - \frac{1}{2} H^2 \underline{n}$, i.e. results solely from the flow of current in the conductors.

Class 2: Classical machines in which the conductors are embedded in slots cut in the ferro-magnetic core. Since most of the flux passes through the teeth, B in the slots is small and so is the force acting on the conductors. The force is predominantly exerted on the tooth sides, where the conductor currents produce a large component $\underline{H} \cdot \underline{n}$.

It follows that the dominant term is $(\underline{M} \cdot \underline{n}) \underline{H}$.

Class 3: variable reluctance machines in which the inequality $(\underline{H}_o - \underline{H}) \cdot \underline{n} \gg \underline{H} \cdot \underline{n}$ prevailed and the dominant term is: $\frac{1}{2} (\underline{M} \cdot \underline{n})^2 \underline{n}$.

B. Efficiency Considerations

At large power levels one of the most important performance parameters is the efficiency η. With the help of dimensional analysis one can reach

the conclusion that with normal conductors the total joule losses are minimized when they are equally divided between the field and the armature. Similarly in iron-cored machines the total volume is minimized where the iron, through which the magnetic fluxes are channeled, and the conductors, through which the electric currents flow, are allocated equal volumes. In that case the joule losses in the conductors predominate over the eddy and hysteresis losses in the iron. With this in mind the various machine classes compare as follows:

Class 1: air-cored machines. The density of power dissipated in the conductors is

$$p_j = \rho J^2 \tag{9}$$

where ρ is the resistivity of the material. The density of power converted is

$$p_c = J B v = J \mu_o H v \tag{10}$$

where v = relative velocity of armature conductor. The ratio(loss/power) is then

$$1 - \eta = r = \frac{p_j}{p_c} = \frac{\rho J}{\mu_o H v} \tag{11}$$

Introducing the relation

$$J = \underline{\nabla} \times \underline{H} \cong H/L \tag{12}$$

where L = characteristic linear dimensions of field coils, we obtain:

$$r = \frac{\rho}{\mu_o v L} = \frac{1}{R_m} \tag{13}$$

where R_m = magnetic Reynolds number is the ratio of the conductor velocity to the diffusion velocity of the electromagnetic field. R_m is an index of the electric loading of the machine, i.e. its armature reaction, since $R_m = 1$ when the active conductor is short-circuited.

We observe that the efficiency is independent of the power density and increases with the velocity and size of the machine.

Class 2: Classical machines. Here the flux density is taken to be equal to the saturation level B_s. The converted power density is

$$p_c = v B_s J \tag{14}$$

The loss/power ratio is

$$1 - \eta = r = \frac{p_j}{p_c} = \frac{\rho J}{B_s v} = p_c \frac{\rho}{B_s^2 v^2} \tag{15}$$

and is a function of the power density, but is independent of the dimensions.

Class 3: variable-reluctance machines. An example of such a machine is the homopolar inductor converter where a simple field coil of linear dimension L excites a large number of pole pieces of linear dimension ℓ. In this case the converted power density can be related to the time rate of change of the magnetic energy density w_m as

$$p_c = \frac{d\, w_m}{d\, t} = \frac{w_m\, v}{\ell} \tag{16}$$

where $w_m = H\, B_s = J\, L\, \omega_s$

so that

$$p_c = J\, B_s\, v\, \frac{L}{\ell} \tag{17}$$

The loss/power ratio is then

$$r = p_c \frac{\rho}{B_s^{\,2}\, v^2}\, \left(\frac{\ell}{L}\right)^2 \tag{18}$$

We observe that variable reluctance machines compare favorably with classical machines with regard to both power density and loss/power ratio. On the other hand the frequency increases as L/ℓ; therefore these machines are best suited for high frequency, or low velocity applications.

Class 4: The classification of converters in terms of the Maxwell stress tensor allows one to deduce the overall performance from local conditions. Therefore, it does not apply to mixed type machines, such as the case of the homopolar and M H D converters, where the armature conductors are not embedded in iron, but the field conductors are. Moreover there exist machines in which the field excitation is produced by permanent magnets or by superconducting magnets. In the latter two cases the operating flux density is not determined by saturation effects, but corresponds to the maximum energy product (B H) max, in the case of permanent magnets, and to the critical value H_c, in the case of superconducting magnets. B is then much smaller than B_s in the former case, and much larger than B_s in the latter. The loss/power ratio is obtained by introducing into Eq. (15) the appropriate value of B.

Similarly, in the case of an iron-cored electromagnet the appropriate B is

$$B = \sqrt{\mu_o\, H\, B_s} = \sqrt{\mu_o\, J\, L\, B_s} \tag{19}$$

The converted power is then

$$p_c = J\, B\, v = \sqrt{\mu_o\, L\, B_s}\, \sqrt{J^3}\, v \tag{20}$$

and the loss/power ratio is

$$r = \frac{\rho}{\mu_o} \sqrt[3]{\frac{\mu_o p_c}{B_s^2 L^2 v^4}} \qquad (21)$$

We observe that r is both a function of p_c and of the dimensions.

C. Technological Limitations

The maximum power density that can be attained with electromechanical power converters is determined by limitations in the mechanical, magnetic, and thermal properties of the materials.

The mechanical limitations manifest themselves in three forms: (1) centrigugal forces in rotating devices, (2) magnetic pressure, and (3) transfer of mechanical power through the shaft. Assuming a mechanical stress somewhat lower than half the tensile strength of steel, i.e. $n = 10^9$ N/m^2 the maximum speed in rotating devices is v = 300 m/sec and the maximum flux density B = 40 T. This limiting value also corresponds to the maximum critical field in superconductors. The construction of force free coils is not practical in electromechanical power converters. However, the limitations arising from magnetic pressure can be alleviated by increasing the surface subjected to stress for a given volume. This is accomplished by the construction of complex machines, such as the imbricated disks realization of the homopolar converter.

The magnetic saturation effects restrict the use of iron cores to B < 2 T.

With regard to the thermal limitations, we can express the maximum heat that can be removed by the cooling fluid per unit volume as

$$q = c \frac{\Delta T}{L} v_f \qquad (22)$$

where c = specific heat

ΔT = maximum allowable temperature rise

v_f = fluid velocity

In steady state, the heat removed must balance the losses, or

$$r p_c = c \frac{\Delta T}{L} v_f \qquad (23)$$

We now express p_c in terms of the limiting condition for mechanical power transfer as

$$p_c = \nu \frac{n v}{L} \qquad (24)$$

where ν is a numerical factor which must be less than one when mechanical power transfer can be achieved. We then have

$$\nu = \left(\frac{c\Delta T}{n}\right)\left(\frac{v_f}{v}\right)\frac{1}{r} = \nu_h \qquad (25)$$

We conclude that the losses can be removed only if $\nu < \nu_h$.

In general we have

$$\frac{c\Delta T}{n} \approx 1 \quad \text{for liquid cooling}$$

$$\frac{v_f}{v} \leq 1 \quad \left(\text{with } \frac{v_f}{v} \approx 1 \text{ in the usual machines}\right)$$

$$\frac{1}{r} \gtrsim 1 \quad \left(\text{with } \frac{1}{r} \approx 1 \text{ in low efficiency machines}\right) \qquad (26)$$

We observe that heat removal becomes the limiting factor only in low efficiency machines which must, then, be operated under pulsed conditions. In all other cases $\nu_h > 1$, and hence mechanical transfer is the limiting factor. This conclusion has been confirmed by others [3].

D. Performance Diagrams

The performance of the various types of converters is conveniently compared in terms of two dimensionless parameters:

(1) θ is the product of the loss/power ratio times the magnetic Reynolds number. It is a measure of the inefficiency of the machine. For the general case, in which the resistivity ρ_a of the armature conductor differs from the resistivity ρ_f of the field conductor, we have

$$\theta = r\frac{u_o v L}{\sqrt{\rho_a \rho_f}} \qquad (27)$$

(2) ν is the previously introduced ratio of the density of converted power to the maximum power density allowed by the mechanical stress on the materials. It is a measure of the mechanical utilization of the materials. For the general case we have

$$\nu = \frac{p_c L}{n v}\sqrt{\frac{\rho_a}{\rho_f}} \qquad (28)$$

In terms of the loss factor θ the various machine classes compare as follows:

Class 1: $\theta = 1$

Class 2: $\theta = \dfrac{u_o n \nu}{B_s^2}$

Class 3: $$\theta = \frac{\mu_o n \nu}{B_s^2} \left(\frac{l}{L}\right)^2$$

Class 4:
$$\begin{cases} \theta = \dfrac{n \nu}{(B H)_{max}} & \text{for permanent magnet excitation} \\ \theta = \dfrac{n \nu}{\mu_o H_c^2} & \text{for superconducting magnet excitation} \\ \theta = \sqrt[3]{\dfrac{\mu_o n \nu}{B_s^2}} & \text{for electromagnet excitation} \end{cases} \quad (29)$$

These relations can be plotted diagrammatically on a logarithmic scale, as shown in Fig. 1. The machines having the best performance appear at the lower right-hand portion of the diagram. For instance, the machine M_o is superior to machine M_1, because it has the same power and better efficiency ($\theta_o < \theta_1$): it is also superior to machine M_2, because it has the same efficiency, but a higher output per unit volume. In contrast with the machines of the classes 1, 2, and 4, which can be represented by single lines, the machines of class 3 occupy a band, because of the variable parameter L/l.

The specific power of a converter can be increased by compensating for the armature reaction and by avoiding iron saturation. As was mentioned in Sec. C, this can be accomplished by increasing the number of the constitutive elements of the converter at the price of increasing its complexity. It is, therefore, interesting to determine the limits for each class above for which a complex construction is indispensable.

According to Eq. (5), the total power crossing a surface S enveloping the converter is:

$$\underline{P} = \int_S \left[\mu \underline{H} \, (\underline{H} \cdot \underline{n}) - \frac{\mu}{2} H^2 \underline{n} \right] \cdot \underline{v} \, ds \quad (30)$$

The surface elements of interest are those for which $\underline{v} \cdot \underline{n} = 0$, so that the total power becomes

$$\underline{P} = B_n H_t S v \quad (31)$$

where B_u = normal component of flux density

H_t = tangential component of magnetic field intensity

Since B_u, H_t, and v are limited for each class, one can only attempt to increase S. For a simple machine

$$S \leq V^{2/3} \quad (32)$$

A machine will be defined as complex if

$$S > \nu^{2/3} \tag{33}$$

The loss/power ratio relations for such complex machines have not been derived here, but can be gleaned from Fig. 1.

We assume that copper with a resistivity $\rho = 2 \times 10^{-8}$ Ω-m is used for both armature and field conductors. The diagram of Fig. 1 then reduces to that shown in Fig. 2. The points of maximum attainable power for each class are indicated by the letter M.

We observe that, for all domains of utilization, there always exists a machine of class 1, or of class 4 with superconducting magnets, or of class 3 whose performance is superior to that of a classical machine. Variable reluctance machines are particularly interesting for low power levels; the air-cored machines are preferable for high powers, while the machines with superconducting magnets occupy an intermediate position.

If one fixes r, and v in addition to ρ, the non-dimensional parameters become

$$\theta = L \sim V^{1/3}$$

$$\nu \sim \rho_c L \sim \frac{P}{L^2} \sim PV^{-2/3}$$

$$\text{so that } V \tilde{=} \theta^3 \text{ and } P \tilde{=} \nu\theta^2 \tag{34}$$

The diagrams of Fig. 3 and 4 are drawn for v = 150 m/s and η = 98% and 90% respectively. We observe that the machines with superconducting magnets are always superior to the classical machines. The air-cored machines become superior to the classical machines, when their power exceeds 1,000 M W for an efficiency of 98% and 10 M W for an efficiency of 90%.

References

1. C. Rioux, "Theorie générale Comparative des Machines Électriques établie à partir des Équations du champ électromagnetique" R.G.E. Tome 79 No. 5, Mai 1970, pp. 415-21.

2. C. Rioux, "Recherche critique d'une forme d'electrotechnique adaptée aux grande puissances" These, Faculté des Sciences de Paris, 1969.

3. C.H. Holley and E.M. Willyoung "Conductor-cooled Rotors For Large Turbine-Generators" CIGRE - 1970, Paris, August 24 - September 2, 1970.

Symbols Used

B	magnetic flux density ($Wb/m^2 = T$)
B_n	normal component of B
B_s	saturation value of B
c	specific heat ($J/kg, {}^{o}K$)
f	force density (N/m^3)
F	force (N)
H	magnetic field intensity (A/m)
H_t	tangential component of H
H_o	value of H in the air
J	current density (A/m^2)
l	length dimension of pole pieces (m)
L	length characteristic of field coils (m)
$\underline{M}$	magnetic polarization vector (A/m)
$\underline{n}$	a vector of unit length normal to a surface S
n	tensile strength (N/m^2)
p_j; p_c	power density (W/m^3) dissipated; converted
P	power (W)
r	loss ratio $(p_j/p_c) = 1 - \eta$
R_m	magnetic Reynold's number: diffusion velocity of EM field/conductor velocity
S	surface bounding a volume V
t	time (seconds)
T	temperature (^{o}K)
v; v_f	velocity (m/s); fluid velocity

V	volume (m^3)
w_m	magnetic energy density (J/m^3)
u	magnetic permeability (H/m)
u_o	magnetic permeability of vacuum ($4\pi \times 10^{-7}$ H/m)
ρ_a; ρ_f	resistivity (Ω - m) of armature; field conductors
η	efficiency of power conversion $\frac{P_c - P_j}{P_c}$
γ	numerical factor, < 1 for mechanical power transfer to be possible
γ_h	maximum value of γ permitting removal of heat loss
θ	loss factor ($r R_m$) measuring inefficiency of a machine

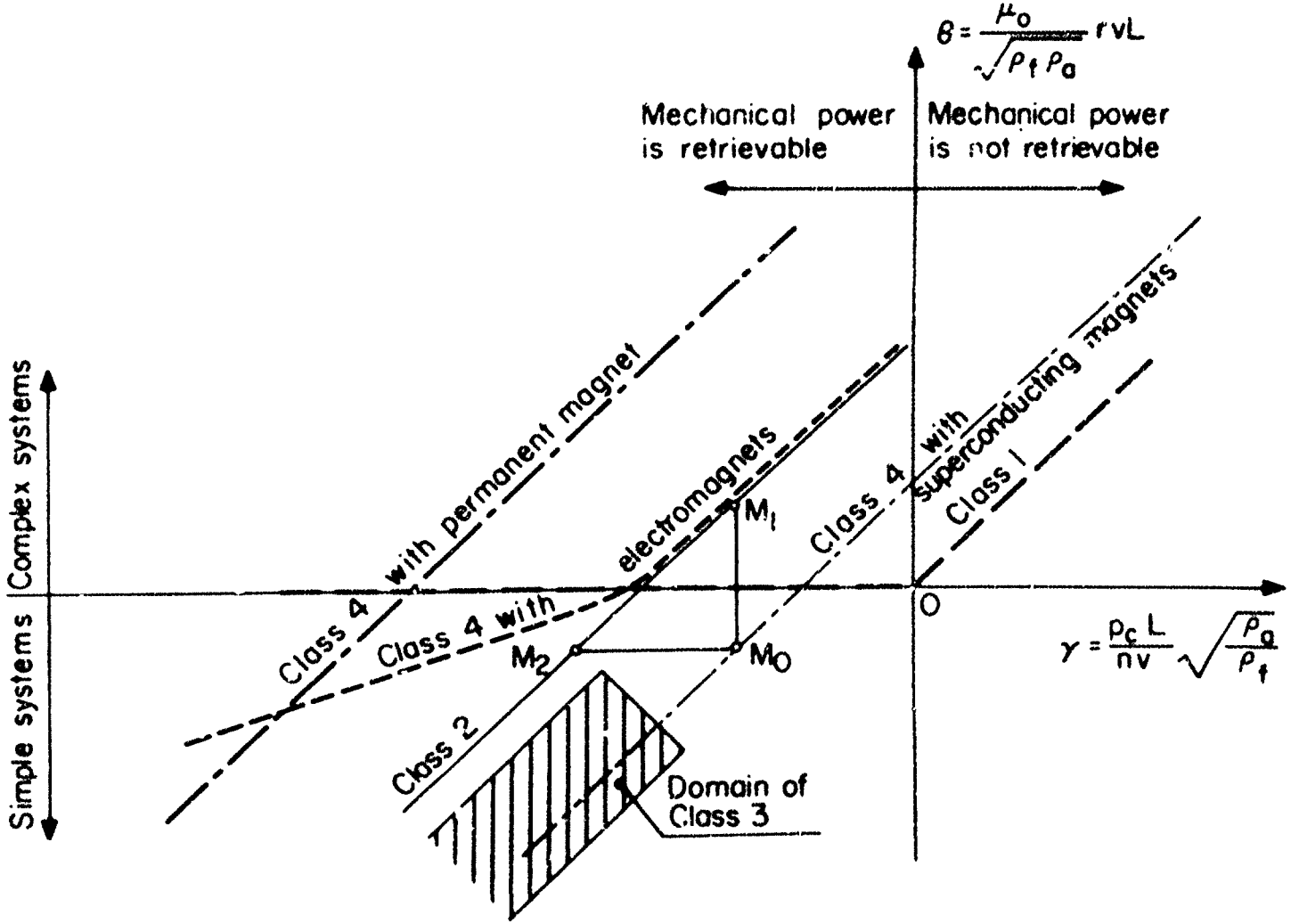

Fig. 1. General performance diagram (Logarithmic scales)

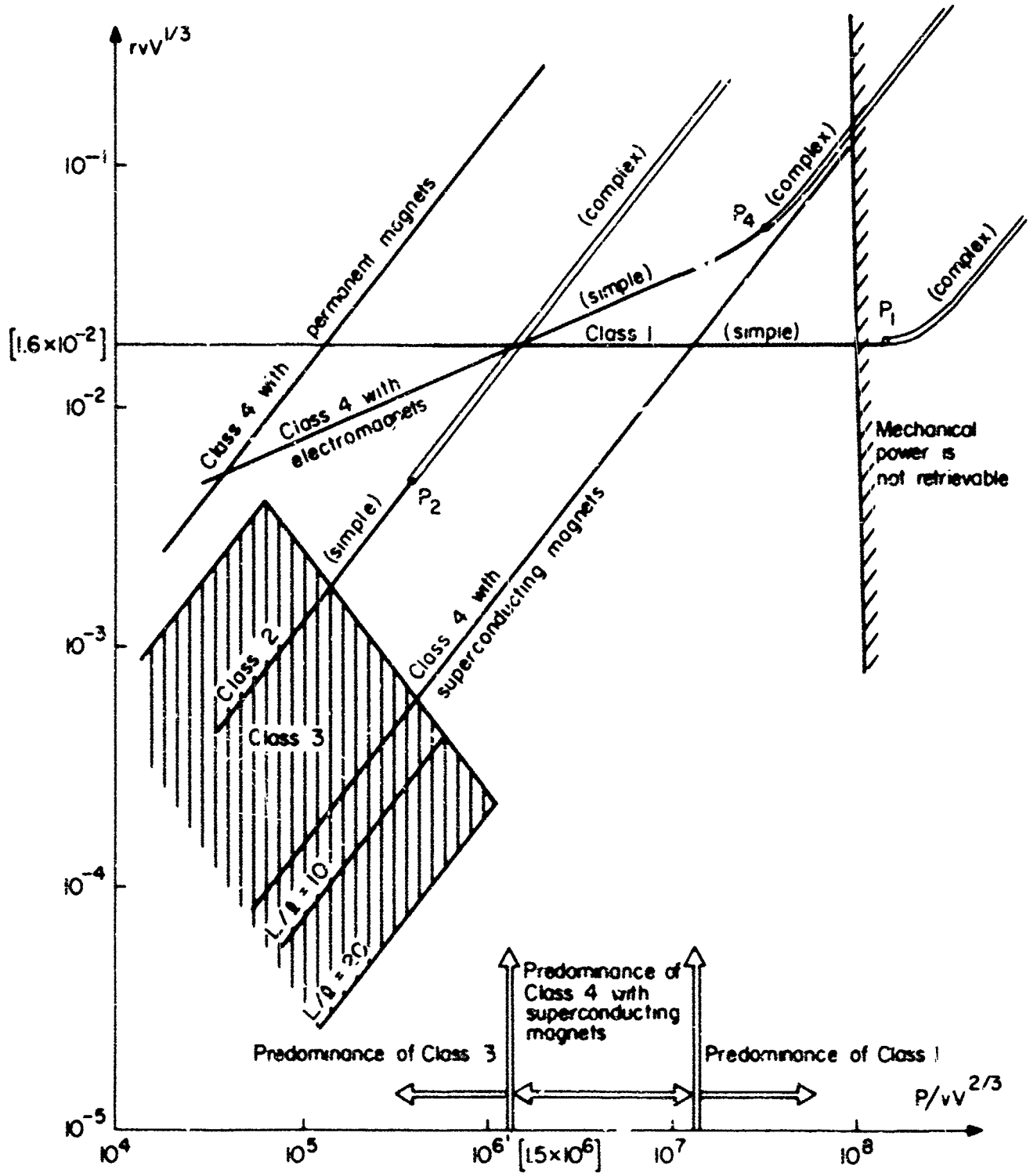

Fig. 2. Performance diagram for machines with copper armature conductors ($\rho_a = 2 \times 10^{-8}$ Ω m)

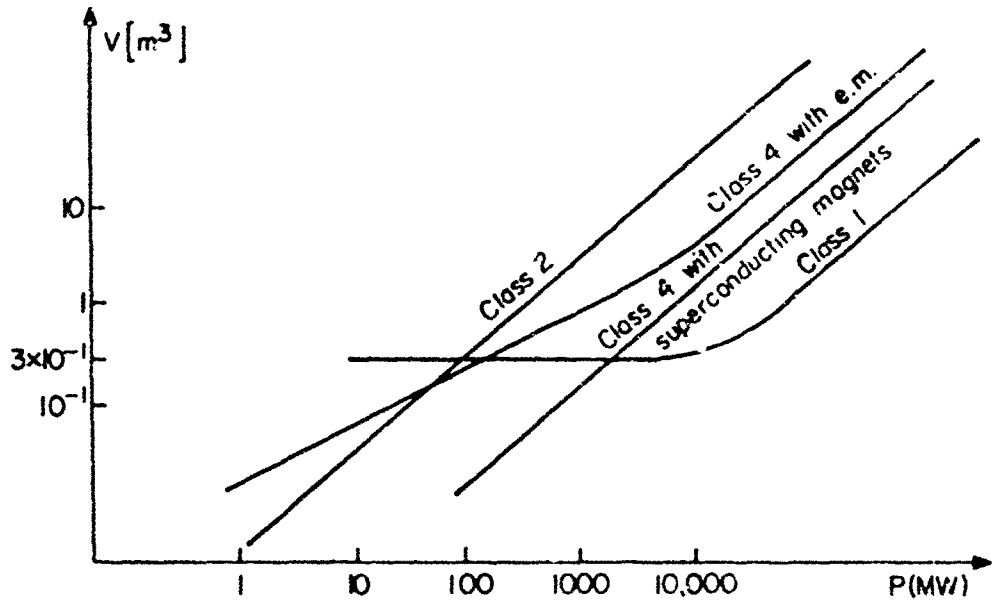

Fig. 3. Performance diagram for $\rho_a = 2 \times 10^{-9}\ \Omega m$, $v = 150$ m/s, and $\eta = 0.98$

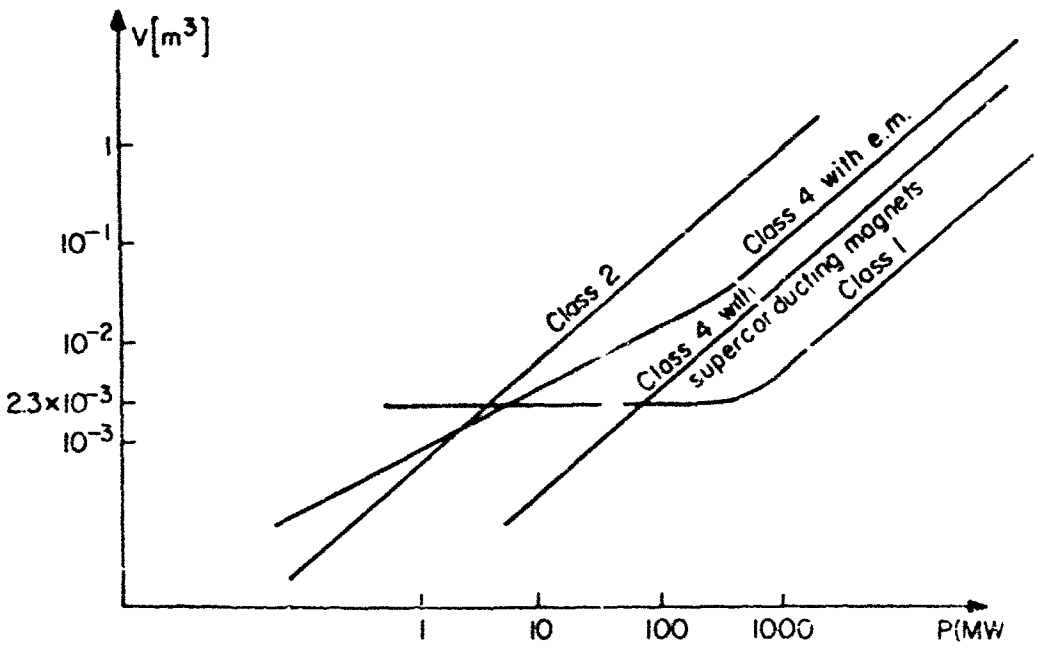

Fig. 4. Performance diagram for $\rho_a = 2 \times 10^{-8}\ \Omega m$ $v = 150$ m/s, and $\eta = 0.9$

VI. Related Topics

A. Switching: Metallization and Non-Ideal Plasmas

1. Introduction - Relevant to the production of high-energy pulses is an understanding of how materials respond to exceptionally high pressures and temperatures. Beyond critical stresses, it is known that phase transitions occur which drastically change their properties. Insight into such phase changes may help to overcome the limitations of present devices, and to suggest new ones. For example, controllable changes from the dielectric to the metallic state, and the reverse could provide the switching mechanisms in pulse generators where they play a crucial role.

2. Pulsers Utilizing Switches - Implosive compression of magnetic fields is one state-of-the-art technique used to generate megajoule pulses. Crawford [1] et al describe one helical coil device (model 129) that delivers 6.6 MA into a load inductance of 70 nH (1.5 MJ) in 44 μ sec "routinely" with the aid of 17 pounds of high explosive. Shearer [2] et al present data for a similar helical coil (design 10) that reliably sends 10 MA pulses into a load of 80 nH (4MJ). They feel that the performance limitations may be associated with the effects of the dense hot gases at the center of the implosion. Magnetic fields of 2 MG, reached during the implosion, correspond to pressures of 160 k bar. Perhaps a knowledge of the thermodynamic and electrical properties of gases at these pressures and higher may be helpful in designing higher-energy generators. Crawford et al were able to achieve an order of magnitude reduction in the pulse rise time. By use of an ingenious switching technique (a combination of an exploding wire fuse and a dielectric breaker switch) they reduced the rise time to 3 μ sec. Perhaps the phase changes mentioned previously could be employed for switching in implosive generators of this type not only for compression of the pulse rise time, but also as a substitute for the mechanical crowbar switches used normally to trap the initial flux at the beginning of the compression period.

   Cascaded flux compression generators have been proposed by Cummings [3], and implementation made possible by his description of an autotransormer that may be used to couple between stages. Here, interstage switching is an important ingredient. In this scheme, the same upper limit to the pulse energy may be set by material stresses associated with megagauss magnetic fields.

   As a last example of pulsers utilizing switches, the ballistic method under investigation by Waniek [4] et al extracts kinetic energy from a projectile by forcing it to do work against magnetic fields of coils. The accumulated magnetic energy is continuously moved forward, from coil stage to coil stage, in anticipation of the arrival of the projectile. Rectifiers in the individual coil circuits serve as switches to successively permit the flux to build up, and then entrap it, for subsequent transfer into the stage ahead.

3. Metallization of Hydrogen - Experiments performed in the USSR, recently reported by Grigor'ev [5] et al, describe the implosive compression of hydrogen. Data obtained for the density in the range 0.4-8 M bar showed an abrupt increase at 2.3 M bar from 1.08 to 1.3 g/cm^3. This discontinuity is consistent with a phase transition from the molecular gaseous state to a metallic state, predicted by many on theoretical grounds. Supporting conductivity measurements were not made. Similar work is being done in the U.S. at Livermore. There is a possibility that metallic hydrogen may be metastable, with stored energy from 30-40 times that of TNT. (In this connection, the intriguing suggestion has been made that such a metastable supercooled state of a dense plasma may occur naturally at normal temperature in the form of a ball of lightning [6]. Metastable states may also be present in the dense plasma bunches which form on the open surface of exploding substances[7]).

4. Phase Transitions in Metal Vapors - In above-critical mercury vapor, non-metal-to-metal transitions have been observed [8]. At 1550° C, increases in pressure from 1.6 - 1.8 k bar are accompanied by density increases from 2-6 g/cm^3 and conductivity increases by a factor of 10^6. In above-critical cesium vapor, non-metal-to-metal transitions were also observed [9] at pressures of the order of 100 bars.

5. Metallization and Non-Ideal Plasmas - When a gas consisting of atoms above the critical temperature is gradually compressed, a state may be reached in which the wave functions of the valence electrons of neighboring atoms overlap each other. The valence electrons are then collectivized (i.e., shared in common) and the substance ceases to consist of atoms only, but, instead, consists of free electrons and ions. This is the essence of the metallization phenomenon.

In ideal plasmas the thermal energy exceeds the energy of Coulomb interaction within a Debye radius $r_D = (\epsilon_o kT/2 e^2 n_e)^{1/2}$. This inequality is reversed in dense plasmas; hence the parameter $\Gamma = (e/4\pi\epsilon_o r_D)/(kT/e)$ serves as an index of nonideality. For experimental study of such dense plasmas, cesium vapor has been a preferred choice because its high atomic weight enables it to be efficiently heated by shock waves, and because it can be easily ionized due to its low ionization potential. A high concentration of charged particles can, thus, be obtained at relatively low temperatures. In recent experiments, the value of $\Gamma = 4$ has been reached [10]. With such large departures from ideality, theories based on the state of an ideal plasma predict a loss of thermodynamic stability. It has been postulated that such a system separates into two phases: a plasma vapor, and a quantized plasma liquid with strong electrostatic interaction between charged particles. The unusual character of the current drop and the anomalous behavior of the resistance in experiments with exploding wires has been associated [11] with the effect of such a plasma-phase transformation, and with the consequent formation of a rarefaction shock. It would be of interest if this conjecture received further experimental confirmation.

Another phenomenon which presents particular interest is an instability which may affect shock fronts propagating in non-ideal plasmas. Such instabilities, leading to what Fortov terms "spontaneous sound emission" may actually prevail in cesium shock tube experiments [12].

6. Theoretical Aspects of Non-Ideal Plasmas - The state of the art with regard to theory leaves much to be desired. From the microscopic point of view a non-ideal (dense) plasma is regarded as a collection of electrons, ions, and atoms interacting via Coulomb forces. In the high density regime, quantum effects play an essential role in determining the thermodynamic properties and the stability of the system. Quantum theories of dense plasmas have not yet been developed to the point where it can reliably be decided whether or not there is a separation into two phases.

The thermodynamic functions of the cesium plasma have been calculated using various approximations to consider the contribution of bound states and the influence of Coulomb interactions [10]. These theories are valid for Γ much less than unity, although some are expected to extrapolate better into the strongly nonideal range than others. For strongly nonideal plasmas the calculation must be made with no separation of the particles into free and bound states [13]. Montecarlo techniques were used to evaluate the configuration integrals. Since in a strongly nonideal plasma it is impossible to exclude the appearance of phase transitions, Norman and Starostin [13] used a method which provided for the possibility of studying them.

We have knowledge from unpublished experimental data [14] that none of the existing theories gives an accurate account of the effects of nonideality on the state of equilibrium and on the ionization balance.

Experimental results [14] show that in the region which is experimentally accessible with cesium vapor, the degree of ionization seems to vary very little with changes in the variables p, ρ, and T despite the great changes that all theories would predict. This could be accounted for by the fact that the effect of an increase in pressure through an increase in the number of free charged particles (the correction in the equation of ionization equilibrium) and the decrease in pressure through the interaction of free particles (the correction in the equation of state) almost completely compensate one another.

Another point of disagreement between theory and experiment [14] involves the density behind the incident wave. Whereas at low pressures that density coincides with the predicted one, at higher pressures it deviates and moves upwards from the isothermic curve by at least 30% (with an experimental error of $\pm$ 10%). This seems to indicate a stronger influence of nonideality upon the equation of ionization equilibrium than upon the equation of state.

Finally, with regard to the state behind the reflected shock, even though the density agrees (within an experimental error of $\pm$ 25%) with the calculations, [14] there are no clear signs of the onset of a phase transformation, even though the nonideality parameter Γ reaches a value of at least 4. In all likelihood, the classical Debye theory predicts a higher degree of interaction, than that which actually takes place.

References

1. Crawford, J.C. and Damerow, R.A., Explosively Driven High-Energy Generators, Journal of Applied Physics, Vol. 39, No. 11, Oct. 1968, pp. 5224-5231.

2. Shearer, J.W.; Abraham, F.F.; Alpin, C.M.; Benham, B.P.; Faulkner, J.E.; Ford, F.C.; Hill, M.M.; McDonald, C.A.; Stephens, W.H.; Steinberg, D.J. and Wilson, J.R., Explosive-Driven Magnetic-Field Compression Generators, Journal of Applied Physics, Vol. 39, No. 4, March 1968, pp 2102-2116.

3. Cummings, D.B., Cascading Explosive Generators with Autotransformer Coupling, Journal of Applied Physics, Vol. 40, No. 10, Sept. 1969, pp. 4146-4150.

4. Waniek, R.W. et al, Chemical to Electromagnetic Energy Conversion Techniques, 2nd Monthly Progress Report, Sept. 18, 1972, under Contract No. F 30602-72-C-0401 for Rome Air Development Center.

5. Grigor'ev, F.V.; Kormer, S.B.; Mikhailova, O.L.; Tolochko, A.P. and Urlin, V.D., Experimental Determination of the Compressibility of Hydrogen at Densities 0.5-2g/cm^3. Metallization of Hydrogen, Zh. ETF Pis. Red., Vol. 16, No. 5, pp. 286-290 (2 Sept. 1972). English translation: JETP Letters, Vol. 16, No. 5, pp. 201-204 (5 Sept. 1972).

   See also New York Times Wed., Jan. 10, 1973, p. 23, Russians Report Brief Conversion of Hydrogen Gas into Metal while under Explosive Compression by Walter Sullivan.

   See also Physics Today, March 1973, pp. 17, 20, Soviet and U.S. Groups seek Hydrogen's Phase by Gloria B. Lubkin.

6. Biberman, L.M. and Norman, G.E., Teplofiz. Vys. Temp., 7, p. 822 (1969).

7. Bauer, A., Cook, M.A. and Keyes, R.T., Proc. Roy. Soc., A, 259, p. 508 (1961).

8. Hensel, F. and Franck, E.U., Metal-Nonmetal Transition in Dense Mercury Vapor, Reviews of Modern Physics, Vol. 40, No. 4, Oct. 1968, pp. 697-703.

9. Alekseev, V.A.; Andreev, A.A. and Prokhorenko, V.Ya., Usp. Fiz. Nauk, 106, pp. 393-426 (1972). English translation: Sov. Phys. Uspekhi, 15, pp. 139-158 (1972).

10. Fortov, V.E., Lomakin, B.N. and Krasnikov, Yu. G., Thermodynamic Properties of a Cesium Plasma, Teplofizika Vysokikh Temperatur, Vol. 9, No. 5, Sept.-Oct. 1971, pp. 869-878. English translation: High Temperature, Vol. 9, No. 5, Sept.-Oct. 1971, pp. 789-797.

11. Bennet, F.D.; Kahil, G.D. and Wedemeyer, E.H., Exploding Wires, (edited by W.C. Chase), Plenum Press, New York, 3, p. 65 (1964), 4, p. 1 (1968).

12. Fortov, V.E., Zh. T.F., 42, pp. 333-335 (1972). English translation: Sov. Phys. Tech. Phys., 17, pp. 264-266 (1972).

13. Norman, G.E. and Starostin, A.N., Teplofiz. Vys. Temp., 8, pp. 413-438, (1970). English translation: High Temperature, 8, pp. 381-408 (1970).

14. Fortov, V.E., Private communication.

Symbols Used

e	Charge of an electron (1.602×10^{-19} C)
k	Boltzmann constant (1.381×10^{-23} J/°K)
n_e	Number of electrons/meter^3
p	pressure (N/m^2)
r_D	Debye radius (m)
T	Temperature (°K)
ϵ_o	Dielectric constant of vacuum (8.85×10^{-12} F/m)
ρ	Density (kg/m^3)
Γ	Index of non-ideality, Coulomb/thermal energy ratio.

VI. B. Comments on Superconductivity

1. Introduction

At the present time, interest in superconducting phenomena and their technological applications is very high. Examples of design studies, experimental devices, experimental large machines and large magnets involving superconductors are listed below to suggest the current degree of activity in this area:

Large Scale Devices and Studies

a. Brookhaven National Laboratory design study of the feasibility of underground transmission of 3-phase 60-cycle power by a superconducting cable system. [1]

b Construction at MIT of an experimental 2 MW 3-phase synchronous generator using a superconducting field winding on the rotor. This follows successful operation of an earlier 45 kW machine. [2]

c. Large magnets [3] - In operation at Argonnes National Laboratory is a 4.8 meter ID, 1.8 WB/m^2, 80 MJ magnet. Under construction for the Batavia National Accelerator Laboratories are 4.26 meter ID, 3 Wb/m^2 coils. Installed at CERN is a 4.6 meter ID, 3.5 Wb/m^2, 800 MJ magnet.

d. A 1-MW MHD generator is under development for the USAF using a $5Wb/m^2$ superconducting magnet. [3]

e. Construction of experimental vehicles for high-speed ground transportation using magnetic levitation with the aid of superconducting coils. [4, 5]

f. Successful operation of a 3250 HP homopolar motor using superconducting windings (in England). Design studies of a superconducting marine propulsion system. [6]

g. Stanford Linear Accelerator: niobium cavities are under development. [7]

Small Scale Devices

a. Use of Josephson junction devices for picosecond switching applications in computers at IBM Watson Research Center. [7]

b. Development of Josephson junction shift registers using magnetic flux quanta as information bits at BTL. [8]

c. Use of Josephson junctions for standardization of the volt at the National Bureau of Standards. [7]

d. Application to the measurement of very small magnetic fields and voltages at low frequencies. [9]

In view of this flurry of activity, it is natural to ask: Is there some way to harness these developments to generate very large pulses of microsecond duration?

Before this question is considered, it would be useful to gain some understanding of superconducting phenomena. With this goal in mind, a brief review is presented of basic ideas and state-of-the-art advances in this area.

2. Normal-Superconducting Transition Temperatures At DC, in the absence of magnetic fields, below a critical temperature, superconducting materials completely lose their resistance. The critical temperature T_c at which this abrupt transition occurs depends on the material. Table I lists T_c for various elements, alloys and compounds [1, 10, 11, 18]. To date, 23.2° K is the highest reported critical temperature [18], obtained for Nb_3Ge.

For thermonuclear research studies, advantage has been taken of the zero-resistance property to construct coils (of Nb3Sn ribbon conductor) operating in the persistent mode [3]; that is, currents once initiated in short-circuited coils are thereafter relied upon to maintain themselves. Powell and Danby of BNL proposed using the persistent mode for magnetic suspension of high-speed ground vehicles, a scheme now being employed to build experimental trains in Japan [4].

3. Effect of Steady Magnetic Field on T_c If "sufficiently small" magnetic fields thread the superconductor, it is found that T_c is reduced. If "sufficiently large" magnetic fields thread the superconductor, it is found that the superconducting state cannot be induced at all. When the superconducting transition occurs with small H, it is coincident with a total expulsion of the magnetic field from the material except for a small sheath. Within this sheath, there is an exponential decrease of H with penetration depth [7] $\delta = \left(\frac{m}{u_o N_s e^2}\right)^{\frac{1}{2}}$ of the order of 1000Å. (m, e are electron mass and charge. N_s is the number of conduction electrons/volume in the superconducting phase.)

Table I

Some Superconducting Materials [1]

		T_c (°K)	H_c (kOe)		Comments
Elements	Pb	7.19	0.8		
	Sn	3.72	0.3	↑	
	Hg	4.15	0.4	Type 1	
	V	5.30	1	-------	
	Nb	9.26	2-20	Type 2 ↓	
Alloys	NbTi	10.0	120	Ductile -	Widely used in US & Europe
	NbZr	10.8	90		
	NbTiZr			Ductile -	Preferred material in USSR & Japan
Compounds	Nb_3Sn	18.3	230	Brittle	
	V_3Ga	15-16	220		
	Nb_3Al	19.3	360		
	V_3Si	17.2			
	$Nb_3Al_xGe_y$	20.7	410		
New Compounds [10, 11, 18]	Nb-C-N	14-18.2		Flexible 6-10 μD filaments	
	Nb_3Ge	22.3			
	Nb_3Ge	23.2			

The critical value of magnetic field H_c above which superconductivity cannot be induced and below which it can is given in Table I [1]. The manner in which the presence of a magnetic field influences the transition temperature is shown in Fig. 1 [12] for Nb_3Sn, a material widely used for magnet construction because of its ability to remain superconducting at very high field values. A similar graph shows magnetic field - temperature envelopes for the 3 classes of superconducting materials [1] (Fig. 2).

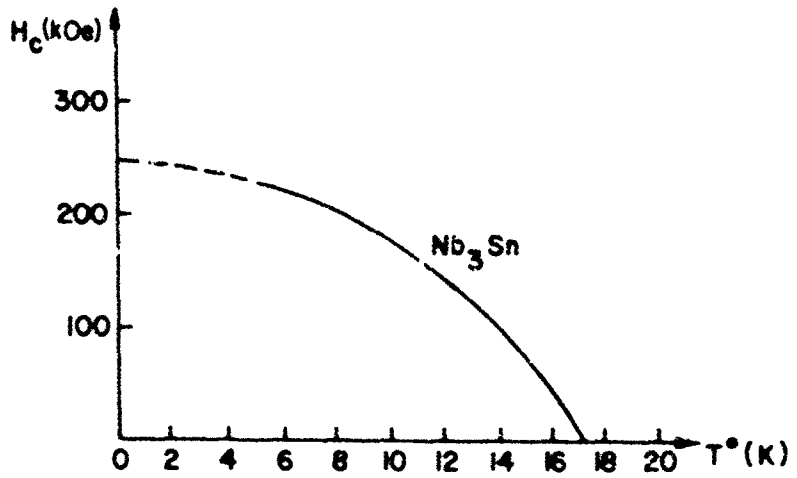

Fig. 1. Dependence of H_c on T

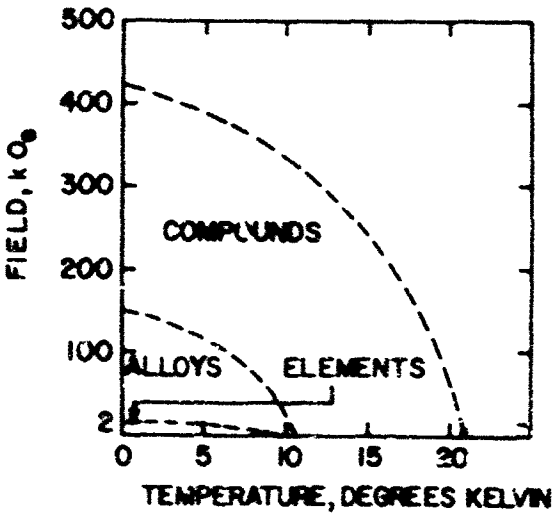

Fig. 2. Temperature vs field envelopes for three types of superconductor.

Behavior in a steady magnetic field serves as the basis for a division of superconductors into two classes.

A low-field superconductor like Pb or Sn is called Type 1. It is characterized by a behavior in magnetic fields as follows: Below H_c, it is a superconductor, with total exclusion of B from the interior of the material. This implies that current flow, when present, must occur in the sheath. If the current is increased sufficiently (in the absence of an externally applied field) to create an $H > H_c$, the conductor discontinuously

reverts to the normal state. In the superconducting state where $H < H_c$, the magnetization characteristic is reversible.

A high-field superconductor like Nb_3Sn is called type 2, because it exhibits the following behavior in magnetic fields: For small $H < H_{c1}$, it totally excludes B from the interior and has a reversible magnetization characteristic. For $H > H_{c1}$ but below H_{c2}, it is still superconducting, but permits limited entry of flux into the interior. Within a homogeneous material, flux quanta form a regular pattern which has been directly observed (see Fig. 3) [13] after being predicted theoretically by Abrikosov [14]. Each flux line site is viewed as the center of a local circulating current or vortex. The range $H_{c1} < H < H_{c2}$ is called the vortex state, accordingly; also the mixed state, since it lies between the superconducting state of type 1 and the normal state. The magnetization characteristic is not reversible in the range $H_{c1} < H < H_{c2}$, but <u>is</u> reversible if $H < H_{c1}$.

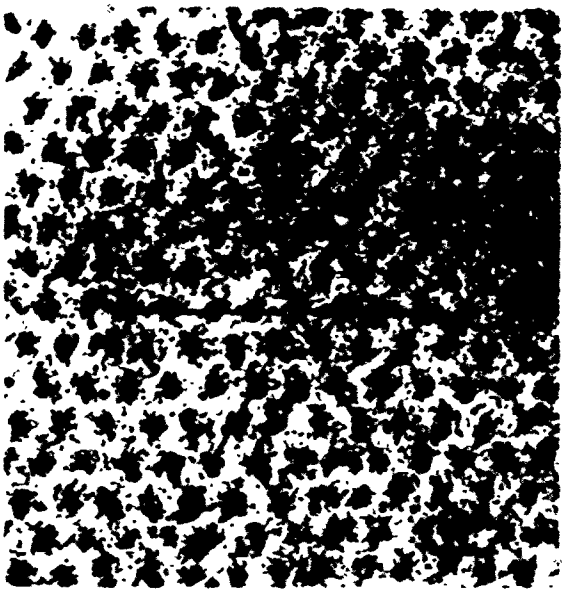

Fig. 3. Flux lattice of a type 2 superconductor, mixed state, with magnetic field normal to the plane of the paper. Each dark spot represents the point of exit of a flux line (which contains one flux quantum) decorated with about 25 ferromagnetic particles for visualization. This is a view of top surface of a Pb-In cylinder B ~ 70 G, T = 1.2 K.

Fig. 3 Flux lattice of a type 2 superconductor, mixed state, with magnetic field normal to the plane of the paper. Each dark spot represents the point of exit of a flux line (which contains one flux quantum) decorated with about 25 ferromagnetic particles for visualization. This is a view of top surface of a Pb-In cylinder B ~ 70 G, T = 1.2° K.

4. Flux Flow The concept of flux flow is a crucial one in the understanding of stability and loss problems in engineering applications of superconductors. A bar of type 2 superconducting material in the vortex state is imagined to carry a current normal to an applied magnetic field, as sketched below [15]:

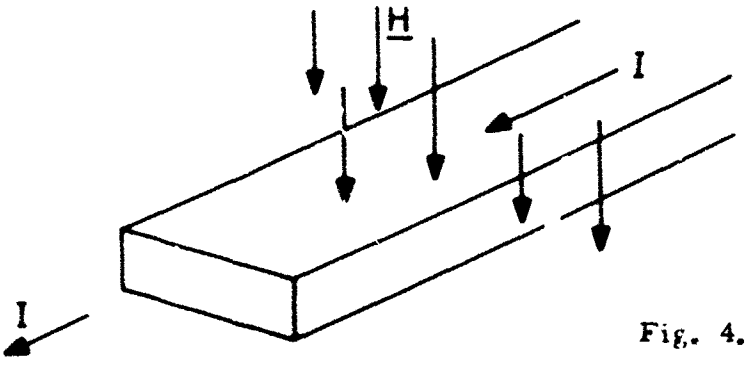

Fig. 4.

Before current was turned on, the flux line pattern is imagined to appear as in Fig. 4. With the transport current flow present, the field outside the bar, on the left, is stronger than that exterior to the bar on the right. Now, the allowable vortex density on the left exceeds that for the 0 current state, whereas it is below the 0 current condition on the right. A drift of vortices from left to right is then to be expected, in view of the vortex gradient and the forces that the flux quanta exert upon each other [14]. This flux flow is a dissipative process [15] when it occurs. It is found, however, that imperfections within the material tend to pin the flux lines by counteracting these forces, preventing free flux flow, and allowing appreciable gradients in vortex density to stably exist across the material (Fig. 5) [13]. Strong enough currents can initiate flux flow by overcoming the pinning forces.

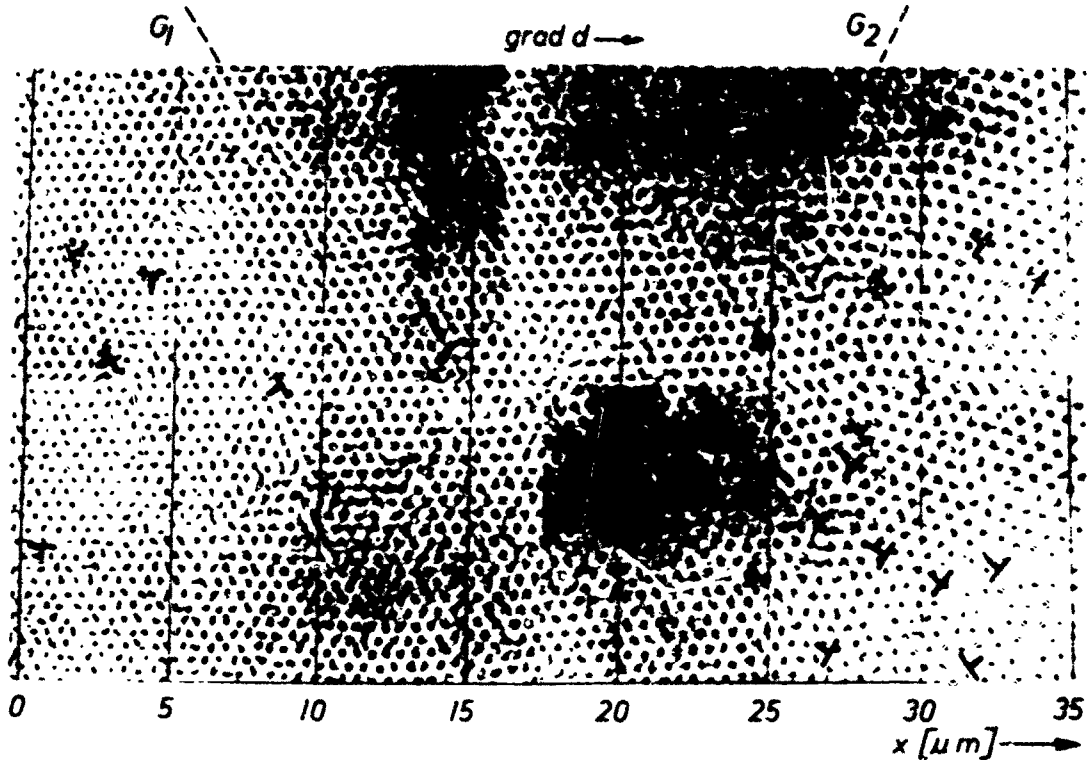

Fig. 5. Area of the flux line lattice with an extremely high, approximately constant flux-line density gradient from right to left. The dislocation cores are indicated by the symbol ⊥.

5. AC Effects For low magnetic field situations, in both Type I and Type 2 superconductors in which no flux penetration has taken place, DC current flow takes place entirely on the surface. If the frequency is raised, losses necessarily exist that increase with frequency. This effect may be quantitatively shown as an equivalent circuit: [7]

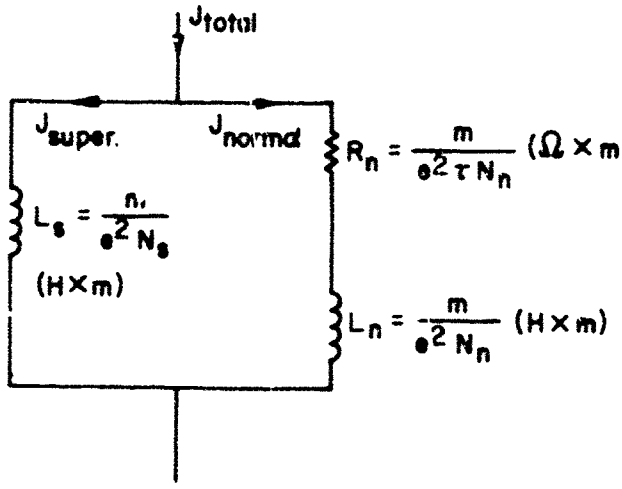

m, e = electron mass, charge

N_n = conduction electrons/ volume in normal state

N_s = conduction electrons/ volume in superconducting state

τ = scattering time for N_n

Use has been made of a 2-fluid model, in which behavior below the transition temperature T_c is accounted for by a combination of normal and superconducting mechanisms.

6. Loss and Stability Mechanisms

A fundamental kind of thermal instability that afflicts superconductors is "flux jumping." Suppose a type 2 superconductor carries a large current. If for some reason there is a small local temperature rise, there will be a reduction of flux-pinning forces and a migration of flux. If the heat generated is not removed quickly enough, additional temperature rise and flux movement occurs. A section of the superconductor can then rise above T_c and can initiate an uncontrolled sudden complete reversion to the normal state.

Stabilization against a catastrophic event of this sort has been achieved by making the superconductor of fine filaments (NbTi, 20 μmD for example) embedded in a copper matrix, as shown in Fig. 6 [7]. The copper serves the dual function of improving thermal conductivity, and providing a bypass current path for a filament if it should become normal until it returns to the superconducting state. Filaments 10 μm in diameter are thought to be intrinsically stable against flux jumping.

The degree of stabilization depends on the relative amounts of copper and superconductor. Full stabilization, which permits complete transfer of current to the copper, is extremely expensive, results in low current densities, and can be used only where total reliability is required. In other situations, partial stabilization is satisfactory.

Relative motion of portions of superconducting windings [3] results in local heat generation. Mechanical rigidity is therefore important to reduce perturbations leading to runaway instabilities.

When time varying external fields or time varying currents are to be transported using superconductors, operation well below T_c is preferred. This is so when viewed in terms of the equivalent circuit above and surface impedance losses because N_s increases and N_n decreases as T is lowered below T_c. In addition, the critical magnetic field H_{c2} increases as T is lowered. Also, at high field levels in type 2 superconductors, varying fields result in hysteresis losses.

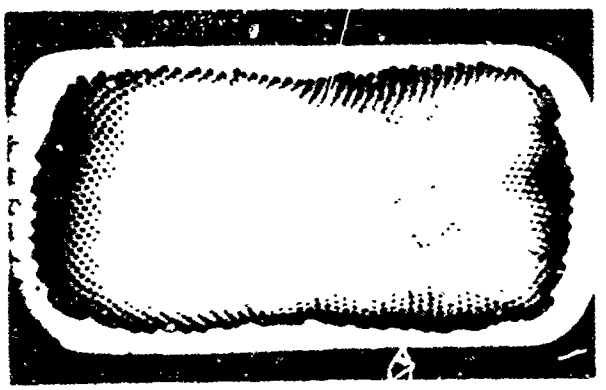

Fig. 6. Cross section of 1.67 - by 3.35 mm Nb-Ti composite containing 2133 strands of Nb-Ti in a copper matrix, with 0.5 twist/inch-capable of carrying 2200 amperes at 6 Wb/m^2. The twist is needed to allow the flux to penetrate into the conductors.

7. Application of superconductivity to pulse generation

Some thought has been given [3, 16] to the use of superconductivity in pulsed systems. This has been done primarily with the idea of reducing the size of a magnetic storage system relative to a capacitive system which might be normally the simplest for delivery of pulses to a load.

From a very general point of view, the task of generating large u second pulses involves storage of electrical energy. Delivery of a 1 terawatt, 1 u second pulse to a load requires an energy transfer of 1 megajoule during the pulse. Energy storage in capacitor banks and in coils [3, 17] is shown conceptually in the diagram, together with the 2 different kinds of switching mechanisms needed.

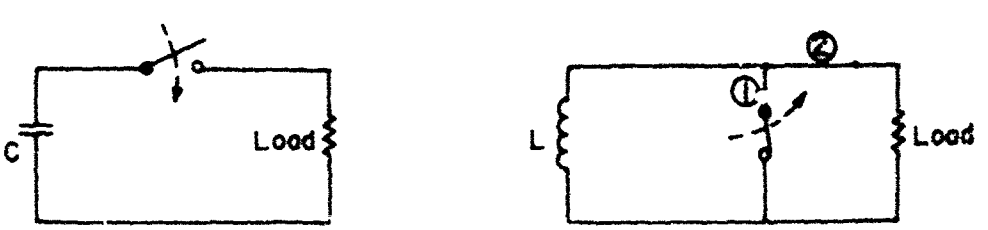

Fig. 7. - Capacitive and Magnetic Energy Storage Systems and their Associated Switching Mechanisms.

In this context, superconductivity can serve to decrease the magnetic energy storage volume; i.e., can increase magnetic energy storage density [3]. Perhaps also the existence of critical magnetic fields in superconducting materials can be used for switching in the magnetic system, thus:

Storage state		⟶	Switched state	
Branch (1)	Superconducting (Low R)		Branch (1)	Normal (High R)
(2)	Normal (High R)		(2)	Superconducting (Low R)

However, even this modest suggestion requires answers to many basic questions. What is the time scale for switching from the superconducting to the normal state within a volume the size of the switch? The picosecond time scales in Josephson junctions may not apply here. It is known that losses occur under transient conditions. But is this an important consideration here? Perhaps the development of an ingenious crowbar using superconductors of the type suggested here can change the present unfavorable outlook for the application of superconductors to narrow pulse generation into a favorable one.

References

1. "Underground Power Transmission by Superconducting Cable," Brookhaven Power Transmission Group, Edited by E.B. Forsyth, March 1972 BNL 50325.

2. J.L. Kirtley, Jr., J.L. Smith, Jr., P. Thullen and H.H. Woodson "MIT-EEI Program on Large Superconducting Machines" Proc. IEEE Vol. 61 No. 1 Jan. 1973 pp 112-115.

3. Z.J.J. Stekly and R.J. Thorne "Large-Scale Applications of Superconducting Coils" Proc IEEE Vol 61 No 1 Jan. 1973 pp 85-95.

4. E. Ohno, M. Iwamoto and T. Yamada "Characteristics of Superconducting Magnetic Suspension and Propulsion for High Speed Trains" Proc. IEEE Vol 61 No. 5 May 1973 pp 579-586.

5. H.H. Kolm and R.D. Thornton "Electromagnetic Flight" Scientific American Vol 229 No 4 October 1973 pp 17-25.

6. A.D. Appleton "Development of Superconducting DC Machines at International Research and Development Co., Ltd." Proc. IEEE Vol 61 No 1 January 1973 pp 106-111.

7. T. Van Duzer and C.W. Turner "Superconductivity: New Roles for an Old Discovery" Spectrum V[illegible] No 12 Dec 1972 pp 53-63.

8. T.A. Fulton, R.C. Dynes and P.W. Anderson "The Flux Shuttle-A Josephson-Junction Shift Register Employing Single Flux Quanta" Proc. IEEE Vol 61 No 1 January 1973 pp 28-35.

9. J. Clarke "Low Frequency Applications of Superconducting Quantum Interference Devices" Proc IEEE Vol 61 No 1 January 1973 pp 8-19.

10. Carborundun Company Final Report under contract F 33615-71-C-1709. Describes the development and behavior of 6-10 micron diameter, flexible fibers of Nb-C-N compounds with T_c from 14-18° K.

11. N.Y. Times "Compound Holds Implications for Superconductivity" Sept. 11, 1973. Article by Victor K. McElheny reports announcements by J. Gavaler of Westinghouse Res. Labs in Pittsburgh, Pa., of a T_c of 22.3° K for Nb_3Ge compound. J.R. Gavaler, "Superconductivity in Nb-Ge films above 22 K." Appl. Phys. Lett. Vol 23 No. 8, 15 October 1973 pp 480-482.

12. S. Foner, E.J. McNeff, Jr., B. T. Matthias, T.H. Geballe, R.H. Willens and E. Corenzwit "Upper critical Fields of $Nb_3(Al_{1-x}Ge_x)$ and Nb_3Al: Measurements of $H_{c2} > 400$ kG at 4.2°K" Physics Letters Vol 31A No. 7 April 1970 p. 349.

13. H. Träuble and U. Essmann "Flux-Line Arrangement in Superconductors as Revealed by Direct Observation" Journal of Applied Physics Vol 39 No 9 Aug. 1968 pp 4052-4059. "Defects in the Flux-Line Lattice of Type 2 Superconductors" Physica Status Solidi Vol 25 1968 pages 373-393.

14. A.A. Abrikosov "On the Magnetic Properties of Superconductors of the Second Group" Soviet Physics JETP Vol 5 No. 6 Dec. 15, 1957 pages 1174-1182. In Russian, JETP Vol 32 June 1957 pages 1442-1452.

15. M.H. Cohen "Superconductivity in Science and Engineering" University of Chicago Press 1968, Chapt. 2, "Superconducting Materials" by T.G. Berlincourt.

16. K.I. Thomassen "Reversible Magnetic Energy Transfer and Storage Systems" Los Alamos Scientific Laboratory, University of California, Informal report LA5087MS, UC-20, dated Nov. 1972.

17. H. Knoepfel "Pulsed High Magnetic Fields" North Holland Publishing Co. 1970 Chapter 6 "Conventional Pulsed Current Generators" pp 130-156.

18. L. Testardi, J. Wernick and W. Royer, post-deadline paper submitted to Symposium on Superconductivity and Lattice Instabilities, Sept. '73, Gatlinburg, Tenn. Reported in Physics Today, Oct. '73, Vol 26 No 10, p. 17, article by R.J. Cohn.

Symbols Used

B	Flux density
C	Capacitance (F)
e	Charge of an electron (1.602×10^{-19} C
H_c	Critical magnetic field strength
I	Current (A)
J	Current density (A/m^2)
$L_{n,s}$	Equivalent sheath inductance (x width) for normal, superconducting currents (H x m)
m	Mass of an electron (9.11×10^{-31} kg)
$N_{n,s}$	Number of electrons/meter^3 in the normal, superconducting phase
R	Resistance (Ω)
R_n	Equivalent sheath resistance (x width) for normal currents (Ω x m)
T_c	Critical temperature (^oK)
δ	Depth of penetration (m)
μ_o	Permeability of vacuum ($4\pi \times 10^{-7}$ H/m)
τ	Scattering time for N_n electrons (s)

VII. An acknowledgment

With humility, the principal investigator wishes to record his thanks for the time and for the gracious help given to him by the following people and their colleagues during his visits to them:

(a) Dr. T.J. Burgess, Lawrence Livermore Lab.

(b) M. Cowan, Sandia Labs.

(c) V.E. Fortov, Moscow Physico-Technical Inst.

(d) Dr. C.M. Fowler, Los Alamos Scientific Lab.

(e) Profs. H. Ikegumi and T. Yamanaka, Inst. of Plasma Physics, Nagoya, Japan.

(f) H. Knoepfel (while at MIT on leave from CERN)

(g) G.E. Norman, A.A. Vedenov and E.R. Velikov, Kuratachov Inst., USSR

(h) Prof. T. Segiguchi, Univ. of Tokyo

(i) A.E. Sheindlin and R.Z. Zagdeev, High Temperature Inst., USSR.

Equally generous of their time were people at the Tokyo Inst. of Technology; Max Planck Inst.; Messerchmitt-Bolkow-Blohm Co. (Munich); Inst. for Theoretical Physics (Innsbruck); Laboratorio Conversione Diretta, Euratom, CNEN (Frascatti); Lebedev Inst.; Moscow State Univ.; Univ. of Leningrad.